Tapping into the antitubercular potential of 2,5-dimethylpyrroles: a structure-activity relationship interrogation

Dorothy Semenya,[‡] Meir Touitou,[‡] Domiziana Masci,[‡] Camila Maringolo Ribeiro,[§] Fernando Rogerio Pavan,[§] Guilherme Felipe Dos Santos Fernandes,[‡,±] Beatrice Gianibbi,[≠] Fabrizio Manetti,[≠] Daniele Castagnolo*[,‡,±]

[‡]School of Cancer and Pharmaceutical Sciences, King's College London, 150 Stamford Street, SE1 9NH, London, United Kingdom. [§]Tuberculosis Research Laboratory, School of Pharmaceutical Sciences, Sao Paulo State University (UNESP), Rod. Araraquara-Jau, km1, 14800-903 Araraquara, Brazil. [≠]Dipartimento di Biotecnologie, Chimica e Farmacia, Dipartimento di Eccellenza 2018-2022, via A. Moro 2, I-53100 Siena, Italy. [±]Current address: Department of Chemistry, University College London, 20 Gordon Street, WC1H 0AJ, London, United Kingdom.

*Corresponding author: daniele.castagnolo@kcl.ac.uk and d.castagnolo@ucl.ac.uk

ABSTRACT

An exploration of the chemical space around a 2,5-dimethylpyrrole scaffold of antitubercular hit compound **1** has led to the identification of new derivatives active against *Mycobacterium tuberculosis* (*M. tuberculosis*) and multidrug-resistant clinical isolates. Analogues incorporating a cyclohexanemethyl group on the methyleneamine side chain at C3 of the pyrrole core, including **5n** and **5q**, exhibited potent inhibitory effects against the *M. tuberculosis* strains, substantiating the essentiality of the moiety to their antimycobacterial activity. In addition, selected derivatives showed promising cytotoxicity profiles against human pulmonary fibroblasts and/or murine macrophages, proved to be effective in inhibiting the growth of intracellular mycobacteria, and elicited either bactericidal effects, or bacteriostatic activity comparable to **1**. Computational studies revealed that the new compounds bind to the putative target, MmpL3, in a manner similar to that of known inhibitors BM212 and SQ109.

KEYWORDS

Tuberculosis, Antimicrobial Resistance, Antimycobacterial, MDR-TB, Pyrrole, SAR

1. Introduction

Tuberculosis (TB) remains a grave global health security threat and is now the second preeminent cause of mortality from a single infectious agent, after COVID-19. The ongoing coronavirus pandemic adds fuel to the fire and may conceivably jeopardise past gains on its containment. According to the latest World Health Organization (WHO) estimates, 10 million people developed TB in 2020 and 1.5 million died (up from 1.4 million deaths in 2019) [1]. Over the years, the rampant emergence of drug resistance in the causative pathogen, *Mycobacterium tuberculosis* (*M. tuberculosis*), has been an encumbrance on global commitments to end TB [2,3]. Current treatment regimens for TB disease rely on combination of mainly decades-old drugs and are associated with suboptimal efficacy, toxicity, long duration and poor adherence which may ultimately lead to drug-resistant cases [4,5]. The treatment of drug-susceptible TB comprises a 2-month initial phase which requires a cocktail of four first-line drugs (isoniazid, rifampicin, ethambutol and pyrazinamide), continued by a 4-month or longer phase involving isoniazid and rifampicin to eliminate dormant bacilli [6,7]. Multidrug-resistant (MDR), pre-extensively drug-resistant (pre-XDR) or extensively drug-resistant (XDR) TB therapy involves much more toxic and expensive drugs and is tainted by a diminished chance of success [8,9]. As evidenced by the latest global data, success rates for the treatment of drug-resistant TB are unsatisfactory (~ 57% for MDR- or rifampicin-resistant TB) in comparison to drug-susceptible cases (~ 85%) [1,8]. Inasmuch as available TB antibiotic therapies have provided some relief, they fall short of curbing the recalcitrance of *M. tuberculosis*, and this highlights the unmet medical need [2,3]. Potential anti-TB agents continue to emerge as reflected by the 2020 global clinical development pipeline which consists of 22 drugs in total; recently updated to 25 drugs in August 2021[1,8,10]. Two candidates (bedaquiline and delamanid) have only recently received accelerated approval for the treatment of drug-resistant forms of TB. More recently, the WHO has recommended pretomanid (a nitroimidazole developed by TB Alliance), under operational research conditions, for the treatment of fluoroquinolone-resistant MDR-TB (pre-XDR) in combination with bedaquiline and linezolid [8,11]. Other drug candidates in the pipeline are either repurposed drugs including levofloxacin, or novel compounds such as diarylquinoline TBAJ-876 (a 3,5-dialkoxypyridine analogue of bedaquiline), ethylenediamine SQ109, and benzothiazinone BTZ043 and its optimized analogue, macozinone; some of these represent previously unexplored targets/pathways and/or new chemical classes [8,10,12]. Although new TB drug treatments are on the horizon, the fact that *M. tuberculosis* not only displays resistance to existing anti-TB

drugs but also to some of the candidates currently undergoing advanced clinical trials, accentuates the need for innovative and intensified drug discovery efforts.

In efforts to expedite the launch of new and effective anti-TB drugs, multiple drug discovery campaigns are homing in on strategies that offer the prospect of capitalizing on previous research gains as opposed to conventional approaches such as target-based high-throughput methods [13–17]. With an eye toward identifying new antibacterial chemical entities, we adopted a molecular hybridization strategy at the outset focusing on the antitubercular 1,5-diarylpyrrole BM212 and the clinical candidate SQ109, by virtue of the fact that both target the mycolic acid transporter protein MmpL3 and they have similar topological distribution of their chemical features as previously revealed by *in silico* modelling [18]. By retaining the rigid scaffold of BM212 as the template and carrying out modifications with respect to the flexible structure of SQ109, we successfully generated distinct sets of hybrids endowed with activity against *M. tuberculosis*, MDR-TB clinical isolates and/or a panel of Gram-positive and Gram-negative bacteria. The investigations were pivotal in identifying the 2,5-dimethylpyrrole scaffold as one of the key features requisite for antimycobacterial activity, wherein further optimization led to the identification of **1** with enhanced potency against *M. tuberculosis* and intracellular mycobacteria (Fig. 1) [18–21].
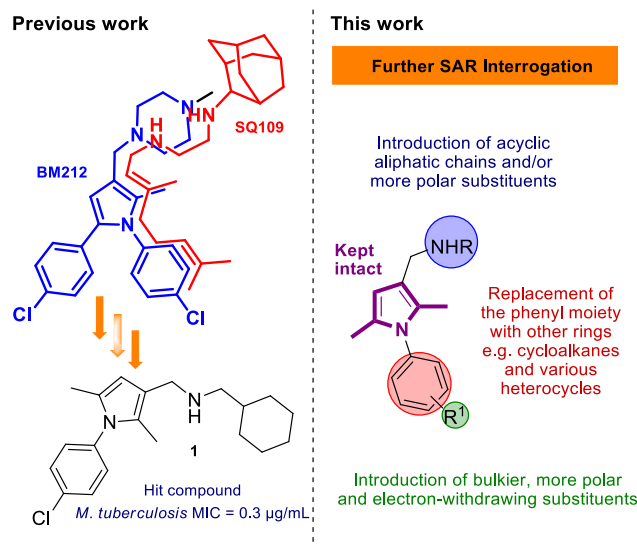

Fig. 1. Rationale behind this work and the strategy adopted in designing analogues of **1**.

Altogether, these findings have provided the impetus for further investigation of **1**. Herein, we report a more extensive structure-activity relationship (SAR) interrogation of **1** with the aim to identify new antitubercular compounds eligible for hit-to-lead development (Fig. 1).

## 2. Results and discussion

2.1. Chemistry

SAR considerations deduced from our previous works only underscored the indispensability of the 2,5-dimethylpyrrole scaffold of **1** to antimycobacterial activity and suggested the benefit of having bulky, aliphatic and lipophilic substituents on the methyleneamine side chain on C3 of the pyrrole [18–21]. On that account, next we sought to expand the scope of the investigation focusing on the N1 position and C3 of the pyrrole nucleus as key sites for diversification (Fig. 1). To better understand the importance of the presence of an *N*-phenyl moiety as determined previously, which may favour π−π interactions and H-bonding with respect to binding to biological targets [20], it was decided to replace it with non-planar puckered cycloalkanes. Furthermore, the *N*-phenyl moiety was replaced with other rings including pyridine to incorporate heteroaromaticity, as well as with more flexible benzyl or picolyl moieties to interrogate whether free rotation at that position has any effect. The synthesis of this series of pyrrole derivatives **5a-r** was achieved through an adaptation of classical synthetic methods as previously reported (Scheme 1 and Table 1) [20,21].

Reagents and conditions: (i) RNH$_2$, PTSA;
(ii) DMF, POCl$_3$; (iii) R^{1}NH$_2$, AcOH, Na(AcO)$_3$BH
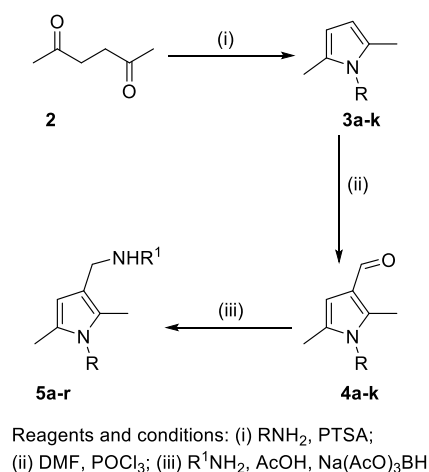
Scheme 1. Synthetic route followed for the synthesis of pyrroles **5a-r**.

The synthetic route started from microwave-assisted Paal-Knorr pyrrole synthesis through condensation of commercially available 2,5 hexadione **2** with the appropriate primary amines. The corresponding pyrroles **3a-k** were then formylated under Vilsmeier-Haack reaction conditions involving an *in situ* generation of the formylating agent from DMF and phosphorus oxychloride. Subsequently, the formylated pyrroles **4a-k** and appropriate amines were subjected to reductive amination using Na(AcO)$_3$BH as a reducing agent to afford the desired analogues **5a-r**. The derivative **5r** was designed as a hybrid of the *N*-phenyl-2,5-dimethylpyrrole scaffold with the antitubercular drug isoniazid. Another set of pyrroles **5s-ab**

was distinctly designed with the aim to impart some degree of hydrophilicity and to further investigate structural diversity at the N1 and C3 positions (Table 1). In essence, either a polar guanidine functional group or a primary amine was introduced on a cyclic or acyclic aliphatic side chain terminating the methyleneamine on C3. In addition, various polar para substituents on the *N*-phenyl ring were explored to determine whether their electronic and steric factors have any preponderant role on activity. The preparation of this series of pyrrole derivatives **5s-ab** was carried out using the synthetic routes described in Schemes 2-5. The synthesis of the pyrroles **5t-x** bearing a guanidine chain involved previous preparation of aminoalkylguanidines **7a-c** from the reaction of 1,3-di-boc-2-trifluoromethylsulfonyl guanidine **6** with the appropriate amine under basic conditions (Scheme 2).

Reagents and conditions: (i) Et$_3$N, RNH$_2$
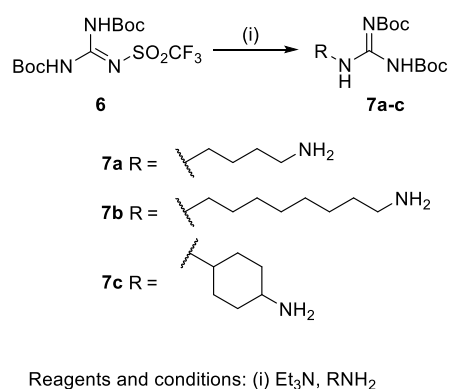
**Scheme 2.** Preparation of aminoalkylguanidines **7a-c**.

The synthesis of derivatives **5v** and **5y** involved an *O*-alkylation of the *N*-phenol moiety of **9** with *tert*-butyl-chloroacetate **10** in the presence of NaI, followed by reductive amination with the appropriate amine and *tert*-butyl or Boc-deprotection using HCl/AcOEt (Scheme 3). The carbaldehyde **13** was obtained from intermediate **12** under Vilsmeier-Haack conditions. Both the formylation of the pyrrole ring and the formation of the dimethyl amide chain were achieved at the same time by treating **12** with POCl$_3$ in DMF. Finally, the reaction of **13** with cyclohexylamine under reductive amination conditions led to derivative **5s,** while its reaction with *di*-Boc-guanidine **7b** followed by Boc-deprotection using HCl/AcOEt afforded **5t** (Scheme 3). Derivatives **5z** and **5aa** were synthesised using a slightly different synthetic route as depicted in Scheme 4. The pyrrole intermediates were obtained through microwave-assisted Paal-Knorr condensation between 2,5-hexanedione **2** and *tert*-butyl-4-aminobenzoate **14** using different organic solvents. Ethanol was used for the synthesis of intermediate **15**, playing a key role as a reagent since it displaced the *tert*-butyl group from **14**, while THF was used to afford intermediate **16**. Subsequently, treatment of both pyrrole intermediates **15** and **16** with

formaldehyde, glacial acetic acid and commercially available cyclohexylamine, under Mannich reaction conditions, afforded the derivatives **5z** and **17**. The final step for the synthesis of derivative **5aa** involved a *tert*-butyl ester-cleavage of **17** with a freshly prepared HCl/AcOEt solution.
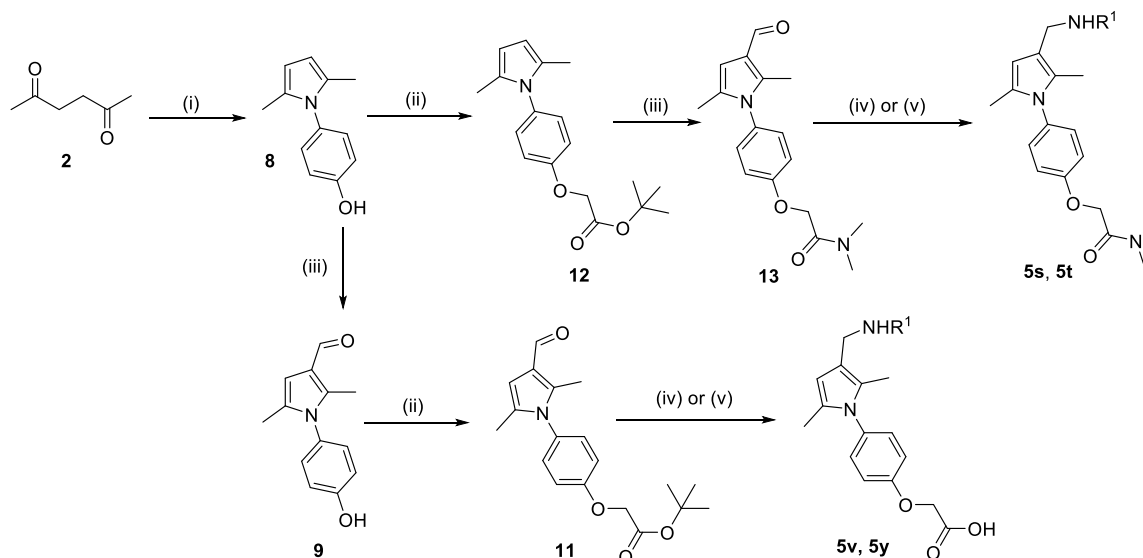
Reagents and conditions: (i) *p*-hydroxyaniline, PTSA; (ii) *tert*-Butyl chloroacetate **10**, K_2CO_3, NaI; (iii) $POCl_3$, DMF; (iv) AcOH, $Na(OAc)_3BH$, cyclohexylamine for **5s** and **5y**; then HCl/AcOEt for **5y** (v) AcOH, $Na(OAc)_3BH$, **7b** for **5t** and **5v**; then HCl/AcOEt.

Scheme 3. Preparation of carbaldehyde intermediates of derivatives **5s-t** and **5v** and **5y**.
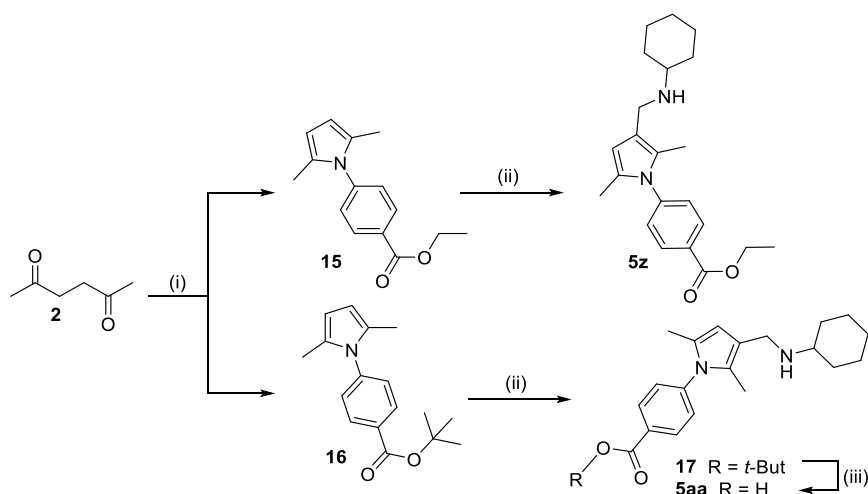
Reagents and conditons: (i) *tert*-butyl-4-aminobenzoate **14**, PTSA, EtOH for **15** or THF for **16**; (ii) cyclohexylamine, CH_2O, AcOH, molecular sieves, THF; (iii) HCl/AcOEt

Scheme 4. Synthesis of derivatives **5z** and **5aa**.

Finally, the guanidine and amino derivatives **5u**, **5w**, **5x** and **5ab** were obtained by following the synthetic route reported in Scheme 5. The aldehyde **4k**, synthesised as previously reported, was reacted with the appropriate Boc-protected amines and guanidines under reductive amination conditions, followed by deprotection in HCl/AcOEt yielding derivatives **5u**, **5w**, **5x** and **5ab** as hydrochloric salts.
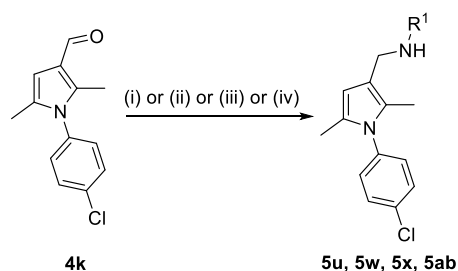
Reagents and conditions: (i) AcOH, Na(OAc)$_3$BH, **7c** for **5u**, then HCl/AcOEt; (ii) AcOH, Na(OAc)$_3$BH, **7a** for **5w**, then HCl/AcOEt; (iii) AcOH, Na(OAc)$_3$BH, **7b** for **5x**, then HCl/AcOEt; (iv) AcOH, Na(OAc)$_3$BH, *N*-Boc-1,4-diaminocyclohexane for **5ab**, then HCl/AcOEt.

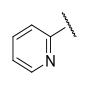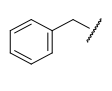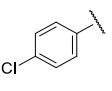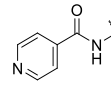**Scheme 5.** Synthesis of derivatives **5u, 5w, 5x** and **5ab**.
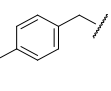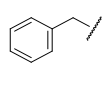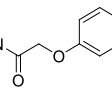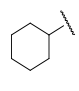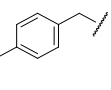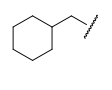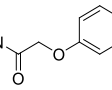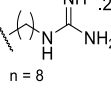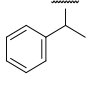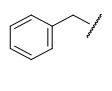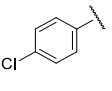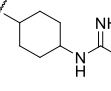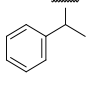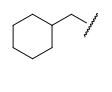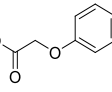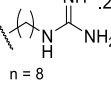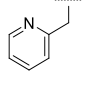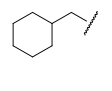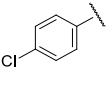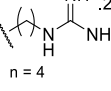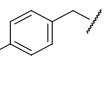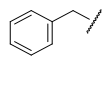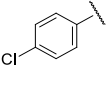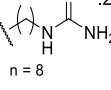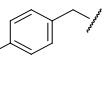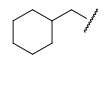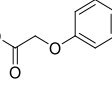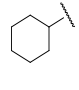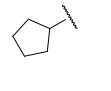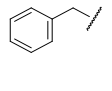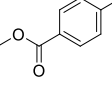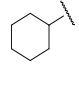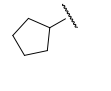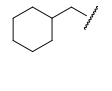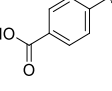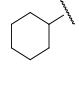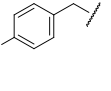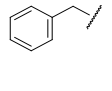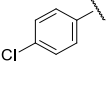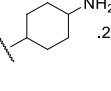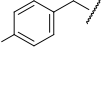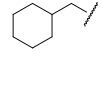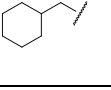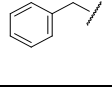
2.2. Biological evaluation

2.2.1. In vitro antimycobacterial activity

The library of pyrrole compounds **5a-ab** was first screened *in vitro* for growth inhibition of *M. tuberculosis* (H37Rv). Generally, the tested compounds exhibited significant antimycobacterial activity with minimum inhibitory concentration (MIC) that inhibited 90% of bacterial growth in the range 0.40->25 µg/mL (Table 1).

Table 1. Structures of the 2,5-dimethylpyrrole derivatives **5a-ab** and their minimum inhibitory concentration (MIC$_{90}$)[a] against *M. tuberculosis* (H37Rv).

Cmpd	R	R^1	MIC$_{90}$ (µg/mL)	Cmpd	R	R^1	MIC$_{90}$ (µg/mL)
5a			1.74±0.28	**5p**			11.17±0.57
5b			16.26±3.80	**5q**			0.40±0.03

Compound			MIC	Compound			MIC
5c			>25	5r			0.49±0.26
5d			10.55±6.28	5s			>25
5e			1.39±0.01	5t			8.91±2.55
5f			7.94±2.81	5u			10.45±3.54
5g			4.48±0.87	5v			13.23±5.49
5h			23.01±2.27	5w			14.24±5.58
5i			5.97±0.33	5x			3.58±0.88
5j			4.88±1.08	5y			16.35±7.02
5k			13.43±3.99	5z			5.14±1.17
5l			9.21±1.63	5aa			>25
5m			6.96±1.29	5ab			>25
5n			0.73±0.01	MOX			0.07 ± 0.01
5o			6.58±1.73	INH			0.19 ± 0.05

[a]The results are mean ± standard deviation of three independent tests; MOX = moxifloxacin, INH = isoniazid. MICs determined *in vitro* by a 96-well microtiter plate assay.

All the derivatives (**5a**, **5e**, **5j**, **5n** and **5q**) bearing a cyclohexanemethyl moiety on the methyleneamine side chain at C3 of the pyrrole nucleus, displayed an MIC_{90} less than 10

µg/mL apart from the *N*-(2-pyridyl)- and *N*-(α-picolyl)-substituted analogues (**5b** and **5h**, respectively). These observations are congruent with our previous SAR deductions [20], and re-emphasize the essentiality of a cyclohexanemethyl group on the methyleneamine side chain while they seem to suggest that a pyridine moiety at the N1 position is unfavourable. Notably, the lowest MIC_{90} values corresponded to compounds with either a cyclohexyl (**5a** 1.74 µg/mL), a 4-chlorobenzyl (**5e** 1.39 µg/mL), a 4-fluorobenzyl (**5n** 0.73 µg/mL) or a 2-benzothiazolyl (**5q** 0.40 µg/mL) ring on the N1 position, thus suggesting that the replacement of the *N*-phenyl group with other rings is to some extent tolerated. Interestingly, analogue **5r**, obtained by molecular hybridization of the *N*-phenyl-2,5-dimethylpyrrole scaffold with isoniazid, displayed the second most potent antimycobacterial activity (0.49 µg/mL). On the other hand, analogues bearing a benzyl moiety on the methyleneamine side chain at C3 (**5d**, **5m** and **5p**) were less potent than their cycloalkyl counterparts, as was foreseeable. The introduction of more polar substituents on the methyleneamine side chain including those incorporating a guanidine functionality generally led to a decrease in antimycobacterial potency, while the derivative **5x** with an acyclic group stood out (MIC_{90} of 3.58 µg/mL). Moreover, the presence of bulkier, more electron-withdrawing and polar groups on the *para* position of the *N*-aryl ring (as exemplified by **5s**, **5y** and **5aa**) in place of a halide substituent, appeared less desirable. Taken together, these SAR results indicate that lipophilicity is positively implicated in the antimycobacterial activity of the **5a-5ab** series. The presence of a pyridine ring on the pyrrole nitrogen as well as of guanidine/amine groups on either the *N*-phenyl ring or the side chain has yielded compounds with lower biological activities, while an increased lipophilicity of the *N*-pyrrole substituents led to more potent derivatives like **5q**.
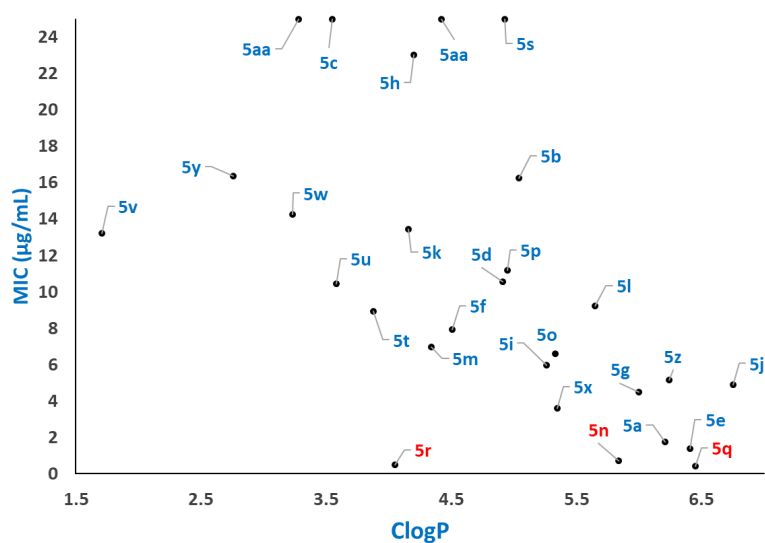
Fig. 2. Correlation between MIC and ClogP values of pyrroles **5a-5ab**. The most active compounds **5n**, **5q** and **5r** are highlighted in red.

A good linear correlation between the ClogP and MIC values of the pyrrole derivatives has been observed in the **5a-5ab** series (Fig. 2), clearly showing that compounds with higher lipophilicity present higher antimycobacterial activity. This direct correlation could partly be attributed to the lipophilic nature of the *M. tuberculosis* cell wall, which allows compounds with higher lipophilicity to permeate more readily and to reach their site of action. Compound **5r**, despite presenting a pyridine ring on its side chain, still showed high antitubercular activity. It is plausible that in this specific case, **5r** behaves like a prodrug releasing isoniazid, which is in turn responsible for the observed MIC.

2.2.2. Cytotoxicity and Selectivity Index (SI)

Pyrrole derivatives displaying an MIC_{90} lower than 10 µg/mL were further tested for cytotoxicity against human pulmonary fibroblasts (MRC-5 cell line - ATCC CCL-171) and murine macrophages (J774A.1 cell line - ATCC TIB-67), and selectivity indices were determined to rule out compounds with potential cytotoxic effects (Table 2). All three best hit compounds (**5n**, **5q** and **5r**) were selective against both cell lines. Compound **5r** showed an excellent SI of 144.86 (macrophages) and 177.29 (fibroblasts), almost 7 times higher than that of the most potent compound **5q**. Analogues **5a**, **5g** and **5i** displayed SI higher than 10 against murine macrophages or fibroblasts, but not against both cell lines. The rest of the compounds including guanidine-incorporating derivatives (**5t** and **5x**) had very low SI values indicative of poor cytotoxicity profiles.

Table 2. Cytotoxicity and selectivity index of selected derivatives against human pulmonary fibroblasts and murine macrophages.

Cmpd	MIC_{90} H37RV (µg/mL)	IC_{50}^{a} ATCC TIB-67 (µg/mL)	SI^{c}	IC_{50}^{b} ATCC CCL-171 (µg/mL)	SI^{c}
5a	1.74	11.99±0.08	6.89	26.70±9.00	15.35
5e	1.39	5.92±0.53	4.25	10.75±1.04	7.71
5f	7.94	17.56±0.71	2.21	33.34±4.94	4.20
5g	6.04	60.64±4.24	13.53	23.44±4.16	5.23
5i	5.58	94.02±5.98	15.75	13.71±2.24	2.30
5j	4.88	25.06±12.12	5.13	15.58±2.57	3.19
5m	6.96	15.69±4.95	2.26	16.16±2.26	2.32

5n	0.73	9.88±3.10	13.57	20.98±10.11	28.82
5o	6.58	13.44±3.91	2.04	18.26±3.26	2.78
5q	0.40	8.47±0.86	21.18	10.31±1.41	25.81
5r	0.49	78.52±8.81	144.86	96.09±1.09	177.29
5t	8.91	12.77 ± 2.81	1.43	36.01 ± 3.02	4.04
5x	3.58	13.02 ± 2.23	3.64	32.43 ± 7.49	9.06
5z	5.14	9.17 ± 0.61	1.78	19.93 ± 1.94	3.87
MOX	0.07	14.56±1.34	208.96	> 100	1434.89

The results are mean ± standard deviation of three independent tests. [a]Cytotoxicity against murine macrophages (J774A.1 cell line - ATCC TIB-67) at 24h; [b]Cytotoxicity against human pulmonary fibroblasts (MRC-5 cell line - ATCC CCL-171) at 24h; [c]Calculated as the ratio between IC_{50} and MIC_{90}.

2.2.3. Activity against drug-resistant M. tuberculosis clinical isolates

Next, selected candidates were screened against a panel of drug-resistant clinical isolates (Table 3). Intriguingly, all compounds retained considerable activity against the MDR-TB and isoniazid-resistant clinical isolates, except for the isoniazid hybrid (**5r** MIC_{90} >25) that displayed the next best activity against *M. tuberculosis* (H37Rv) and the least cytotoxic effects. The hybrid **5r** showed no activity against the drug-resistant strains, thus indirectly supporting the hypothesis that it may act as a prodrug releasing isoniazid inside the mycobacterial cells following hydrolysis. Among the tested analogues, **5g**, **5i** and **5n** demonstrated the most superior overall activity.

Table 3. MIC_{90} (µg/mL) of selected analogues and clinical antibiotics against *M. tuberculosis* (H37Rv) and five drug-resistant clinical isolates.[a]

Cmpd	H37Rv	CF16 I	CF61 II	CF76 III	CF152 IV	CF161 V
5g	6.04±0.22	8.70±2.87	10.15±2.61	9.13±2.91	4.32± 5.91	9.94±1.48
5i	5.58±0.24	7.51±3.26	9.16±2.03	8.18±2.21	6.35±0.66	6.12±0.07
5n	0.73±0.58	7.69±3.39	9.38±2.40	18.80±6.37	7.53±2.05	7.31±2.21
5q	0.40±0.16	20.11±2.72	23.51±0.90	19.62±6.43	10.93±1.07	13.62±5.00
5r	0.49±0.26	> 25	>25	>25	>25	>25
RIF	0.05±0.03	0.20±0.12	>25	>25	>25	>25
INH	0.11±0.01	>25	>25	>25	>25	>25
MOX	<0.098	0.14±0.03	0.27±0.16	0.20±0.10	0.57±0.13	0.17±0.02
AMK	0.25±0.08	0.22±0.12	0.91±0.36	0.25±0.09	0.19±0.13	0.24±0.08

Classification	Sensitive strain	Resistant to isoniazid	MDR-TB	MDR-TB	MDR-TB	MDR-TB

RIF = rifampicin; INH = isoniazid; MOX = moxifloxacin; AMK = amikacin. [a]The MIC was determined by a 96-well microdilution assay and resazurin was used as an indicator of bacterial viability. The results are mean ± standard deviation of three independent tests.

2.2.4. Time-kill kinetics

A time-kill assay was then conducted in order to determine whether the best compounds were bactericidal or bacteriostatic [22]. The mean of the untreated control at day 12 was 7.54 Log_{10} CFU/mL (Fig. 3). Thus, for a compound to be considered bactericidal it should have a count lower than 4.54 Log_{10} CFU/mL, which represents 99.9% reduction of the bacterial inoculum. All the compounds were evaluated at 1 x MIC, only **5g** (3.94 Log_{10} CFU/mL) and **5i** (2.65 Log_{10} CFU/mL) were considered bactericidal, while the others (**5n**, **5q** and **5r**) presented a bacteriostatic effect. At the concentration tested (0.07 µg/mL), moxifloxacin showed no inhibition of mycobacterial growth. However, it is worth mentioning that usually the bactericidal/bacteriostatic action is concentration-dependent and this further highlights the great potential of **5g** and **5i** [23].
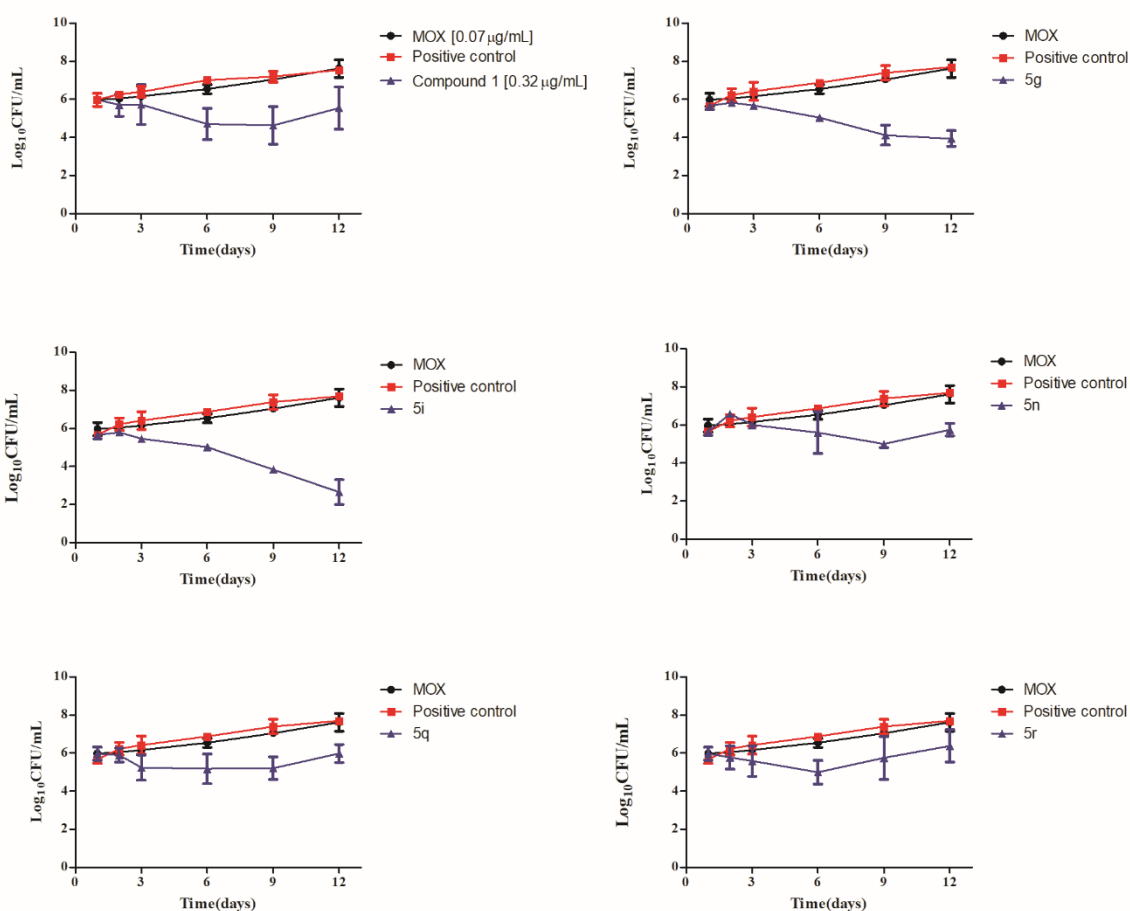
Fig. 3. Time-kill of *Mycobacterium tuberculosis* challenged with the compounds: **1** (0.32 µg/mL), **5g** (4.48 µg/mL), **5i** (5.97 µg/mL), **5n** (0.73 µg/mL), **5q** (0.40 µg/mL), **5r** (0.49 µg/mL), and Moxifloxacin (MOX) (0.07 µg/mL).

2.2.5. Activity against intracellular M. tuberculosis

Given that *M. tuberculosis* has the ability to survive and replicate within macrophages [24], the compounds that exhibited an all-round superior biological profile, including significant antimycobacterial activity against either drug-sensitive or drug-resistant *M. tuberculosis* clinical isolates as well as low cytotoxicity, were further assessed for their ability to penetrate cell membranes and inhibit intracellular bacilli. In general, the compounds exhibited moderate to remarkable growth inhibition of intramacrophagic *M. tuberculosis*, with the exception of **5i** bearing a benzyl group on the methyleneamine side chain (Fig. 4).
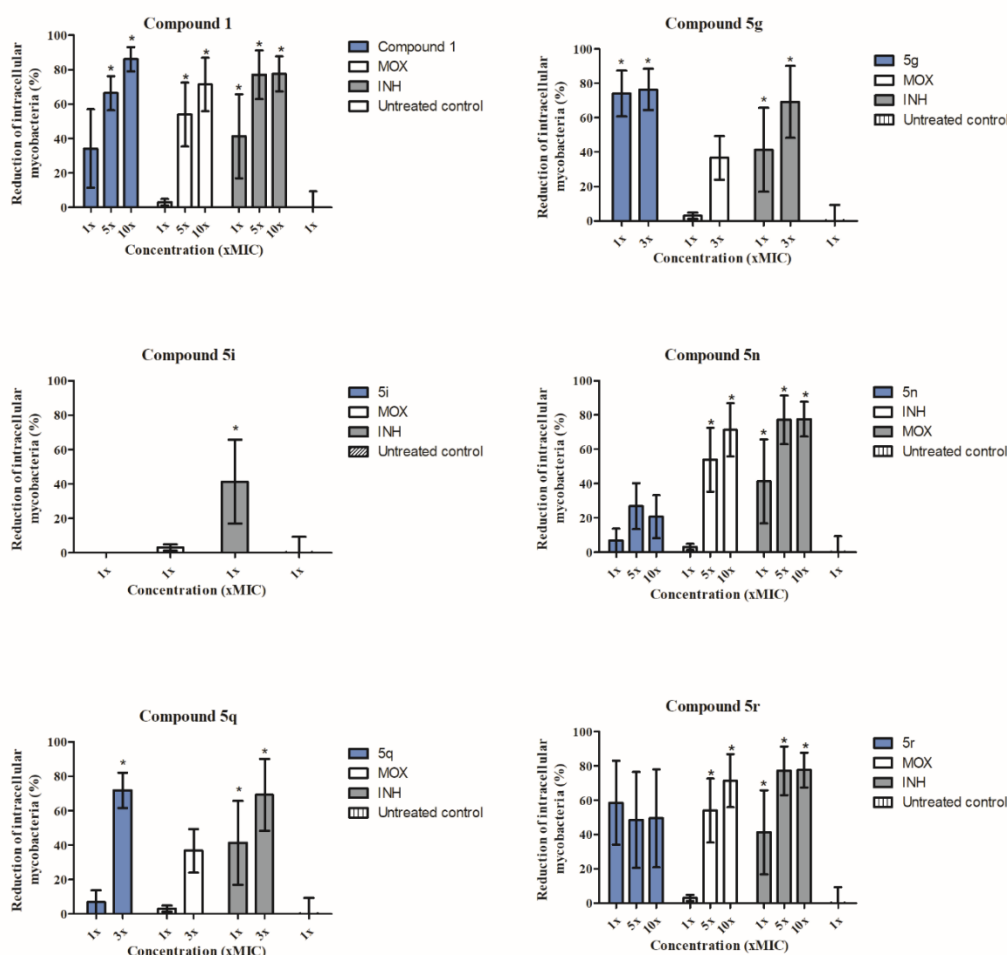
Fig. 4. Reduction of intracellular *M. tuberculosis* (murine macrophages - cell line J774A.1) (%) treated with compound **1**, **5g**, **5i**, **5n**, **5q** or **5r** compared to untreated control (right side). * Significantly different from the untreated control according to one-way ANOVA with Dunnett's post-test ($p<0.05$); MOX = moxifloxacin; INH = isoniazid.

Furthermore, in some instances, their intramacrophagic activity exceeded that of reference antibiotics isoniazid and moxifloxacin. It is worth mentioning that the change in the percentage of inhibition of intracellular bacilli for both **5g** and **5q** were the best results in this evaluation, unfortunately higher concentrations could not be tested due to cytotoxicity.

2.3. Molecular docking

Finally, molecular docking simulations were carried out to rationalise the activity profiles observed. Having designed the pyrrole series using the drugs SQ109 and BM212 as templates, a similar mode of action, namely, inhibition of the mycolic acid transporter MmpL3, was hypothesised. The cryo-EM structure of MmpL3 from *M. tuberculosis* [25] was used to perform molecular docking simulations to find the putative binding mode of the new pyrroles (Figs. 5 and S1, Table S1). The structure of BM212 and SQ109 were used for comparison. In agreement with previous results, the new pyrroles were able to occupy the same binding pocket on *M. tuberculosis* already described for SQ109, BM212, and our previous hybrid pyrroles [20], and showed two alternative binding poses that were different in terms of docking scores.
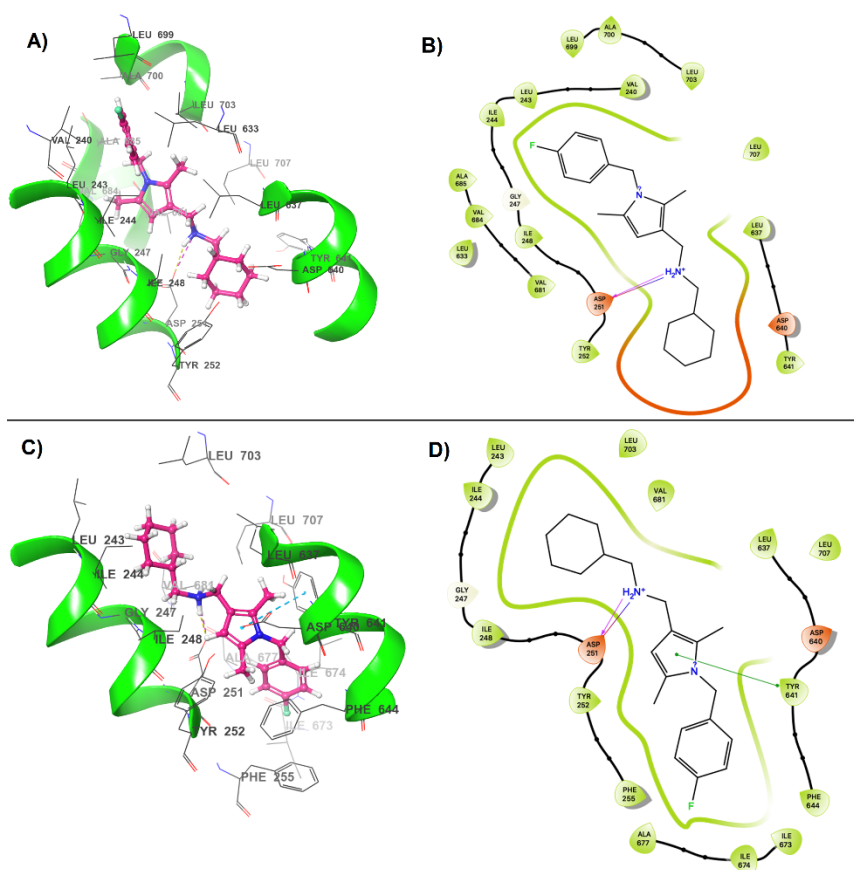
Fig. 5. Docking poses of pyrrole **5n** into the cryo-EM structure of MmpL3 from *Mycobacterium tuberculosis*. A) The *N*-aryl substituent is accommodated within a hydrophobic pocket defined by Leu243, Leu699, Ala700, Leu703, and Leu637, while the cyclohexyl ring at the opposite edge is located within another hydrophobic pocket delimited by Tyr252, Tyr641, and Phe644. Asp251 and the basic nitrogen atom of **5n** give a charge-reinforced hydrogen bond; B) A ligand interaction diagram showing the interaction between the binding site and **5n**; C) Alternative binding pose of the inhibitor within the same binding site. Positions of the terminal edges of **5n** undergo a reciprocal replacement within the two hydrophobic pockets of the binding site; D) A ligand interaction diagram showing the interaction between the binding site and the alternative binding pose of **5n**.

The most representative pose for pyrrole **5n** was characterized by the *N1*-aryl moiety within a hydrophobic pocket defined by Leu243, Leu699, Ala700, Leu703 and Leu637 (Figs. 5A and 5B). Moreover, the C3 side chain at the opposite molecular edge was located within another hydrophobic pocked delimited by Tyr252, Tyr641, and Phe644. Lastly, a charge-reinforced hydrogen bond between the Asp251 side chain and the basic protonatable amino group at the C3 of the inhibitors was an additional common interaction. An alternative pose of **5n** showed an opposite orientation of the phenyl and cyclohexyl molecular edges within the two hydrophobic pockets. An additional π–π stacking between the pyrrole nucleus and the phenyl ring of Tyr641 was also found in the alternative orientation (Figs. 5C and 5D). These results from docking simulations clearly suggested that the new pyrroles could be able to bind a pocket within the MmpL3 structure.

3. Conclusions

A series of new 2,5-dimethylpyrroles designed as analogues of **1** were subjected to phenotypic whole-cell screening which revealed their inhibitory potency against *M. tuberculosis*. Three hits (**5n**, **5q** and **5r)** showed high activity with an MIC_{90} below 1 µg/mL, as well as low cytotoxicity against macrophages and pulmonary fibroblasts. Furthermore, the most active derivatives demonstrated promising activity against a panel of MDR-TB clinical isolates, notable growth restriction of intracellular *M. tuberculosis*, and presented either bacteriostatic or bactericidal effects at 1 x MIC. Derivative **5r** showed an excellent activity against *M. tuberculosis* and a high SI of about 145 and 177 against macrophages and pulmonary fibroblasts, respectively. However, the low activity of **5r** against MDR-TB clinical isolates suggests that it may be a prodrug of isoniazid. Finally, molecular docking studies have been carried out on MmpL3 as the plausible target of the new pyrroles, which suggested a binding mode similar to that of the parent drugs BM212 and SQ109. In conclusion, this work provided an extensive SAR study on 2,5-dimethylpyrrole compounds, highlighting the key functional groups needed for antitubercular activity against wild-type, MDR and intracellular

mycobacteria. Three compounds, **5n**, **5q** and **5r**, together with the hit pyrrole **1**, will be used in follow-on pre-clinical studies.

4. Experimental section

4.1. Chemistry

4.1.1. General

All reagents and solvents were purchased from commercial suppliers and utilized without further purification. Chemical reactions were carried out under a nitrogen atmosphere in over-dried glassware unless stated otherwise. The reactions were monitored by TLC using commercially available pre-coated plates and visualized with UV light at 254 nm; $KMnO_4$ was used to reveal the products. Flash column chromatography was carried out using Sigma Aldrich silica gel (particle size 40-63 µm, pore size 60 Å). ^{1}H NMR and ^{13}C NMR spectra were recorded with a Bruker Ascend 400 spectrometer, at room temperature (rt) operating at the frequencies indicated. Chemical shifts are expressed in parts-per-million (ppm) relative to the internal solvent peak or tetramethylsilane (TMS). Coupling constants (*J*) are reported in Hertz (Hz). Spin multiplicities are denoted by the following abbreviations and combinations thereof: s (singlet), d (doublet), t (triplet), q (quartet), m (multiplet) and br (broad). HPLC analysis was carried out using a Perkin-Elmer 1100 HPLC system coupled with UV/Vis set to 254 nm. HRMS (high-resolution mass) were measured on a Thermo Q-Exactive mass spectrometer with an ESI source. Compounds **3a**, **3c-e** and **4b-c** were synthesized according to previously described methodologies [26–31]. All final compounds showed >95% purity, determined by HPLC analysis, before being submitted for biological assays.

4.1.2. General procedure for the synthesis of pyrroles **3**, **8**, **15** and **16**. The pyrrole scaffolds were synthesized as described in the literature [19,32].

4.1.2.1. 1-cyclohexyl-2,5-dimethyl-1H-pyrrole (3a). (Used in the next step without further purification)

4.1.2.2. 2-(2,5-dimethyl-1H-pyrrol-1-yl)pyridine (3b). Yield: 36%. ^{1}H NMR (400 MHz, CDCl$_3$) 8.46-8.44 (m, 1H), 7.67-7.63 (m, 1H), 7.13-7.11 (m, 1H), 7.07-7.05 (d, *J* = 7.9 Hz, 1H), 5.77 (s, 2H), 2.00 (s, 6H) ppm. ^{13}C NMR (100 MHz, CDCl$_3$) δ 151.8, 149.1, 137.7, 128.2, 122.1, 121.7, 106.7, 12.9 ppm.

4.1.2.3. 1-(4-chlorobenzyl)-2,5-dimethyl-1H-pyrrole (3c). (Used in the next step without further purification)

4.1.2.4. 2,5-dimethyl-1-(1-phenylethyl)-1H-pyrrole (3d). (Used in the next step without further purification)

4.1.2.5. 2-((2,5-dimethyl-1H-pyrrol-1-yl)methyl)pyridine (3e). (Used in the next step without further purification)

4.1.2.6. 2,5-dimethyl-1-(4-methylbenzyl)-1H-pyrrole (3f). Yield: 80%.^{1}H NMR (400 MHz, CDCl$_3$) δ 7.13 (d, *J* = 6.0 Hz, 2H), 6.82 (d, *J* = 9.0 Hz, 2H), 5.89 (s, 2H), 5.00 (s, 2H), 2.34 (s, 3H), 2.17 (s, 6H) ppm. ^{13}C NMR (100 MHz, CDCl$_3$) δ 136.4, 135.4, 129.3, 127.8, 125.5, 105.2, 46.4, 20.9, 12.4 ppm.

4.1.2.7. 1-cyclopentyl-2,5-dimethyl-1H-pyrrole (3g). Yield: 42%. ^{1}H NMR (400 MHz, CDCl$_3$) δ 5.95 (s, 2H), 4.74-4.70 (m, 1H), 2.49 (s, 6H), 2.25-2.08 (m, 6H), 1.90-1.85 (m, 2H) ppm. ^{13}C NMR (100 MHz, CDCl$_3$) δ 128.1, 106.2, 56.4, 31.4, 25.2, 14.3 ppm.

4.1.2.8. 1-(4-fluorobenzyl)-2,5-dimethyl-1H-pyrrole (3h). Yield: 68%. ^{1}H NMR (400 MHz, CDCl$_3$) δ 7.00-6.95 (m, 2H), 6.85-6.81 (m, 2H), 5.85 (s, 2H), 4.96 (s, 2H), 2.13 (s, 6H) ppm. ^{13}C NMR (100 MHz, CDCl$_3$) 162.9, 134.0, 127.7, 127.0, 115.5, 105.4, 45.9, 12.2 ppm.

4.1.2.9. 1-(cyclohexylmethyl)-2,5-dimethyl-1H-pyrrole (3i). Yield: 41%. ^{1}H NMR (400 MHz, CDCl$_3$) δ 5.77 (s, 2H), 3.55-3.54 (d, *J* = 7.1 Hz, 2H), 2.21 (s, 6H), 1.74-1.63 (m, 7H), 1.21-1.17 (m, 4H) ppm.

4.1.2.10. 2-(2,5-dimethyl-1H-pyrrol-1-yl)benzo[d]thiazole (3j). Yield: 43%. ^{1}H NMR (400 MHz, CDCl$_3$) δ 7.60-7.54 (m, 2H), 7.34-7.32 (td, *J* = 7.7 Hz, 1H), 7.16-7.12 (m, 1H), 5.30 (s, 2H), 2.19 (s, 6H) ppm.

4.1.2.11. 1-(4-chlorophenyl)-2,5-dimethyl-1H-pyrrole (3k). Yield: 43%. ^{1}H NMR (400 MHz, CDCl$_3$) δ 7.46 (d, *J* = 8.8 Hz, 2H), 7.20 (d, *J* = 8.7 Hz, 2H), 5.92 (s, 2H), 2.05 (2 s, 6H) ppm. ^{13}C NMR (100 MHz, CDCl$_3$) δ 133.4, 129.3, 128.8, 105.9, 77.0, 76.7, 13.0 ppm.

4.1.2.12. 4-(2,5-dimethyl-1H-pyrrol-1-yl)phenol (**8**): Yield 76%. ^{1}H NMR (400 MHz, CDCl$_3$) δ 7.07 (d, *J* = 8.8 Hz, 2H), 6.89 (d, *J* = 8.8 Hz, 2H), 5.88 (s, 2H), 5.18 (br. s, 1H), 2.01 (s, 6H) ppm. ^{13}C NMR (100 MHz, CDCl$_3$) δ 155.1, 132.0, 129.6, 129.2, 115.9, 105.4, 13.1 ppm.

4.1.2.13. ethyl 4-(2,5-dimethyl-1H-pyrrol-1-yl)benzoate (15). Yield: 72%. ^{1}H NMR (400 MHz, CDCl$_3$) δ 8.16 (d, *J* = 8.7 Hz, 2H), 7.29 (d, *J* = 8.6 Hz, 2H), 5.93 (s, 1H), 4.42 (q, *J* = 7.1 Hz, 2H), 2.05 (s, 6H), 1.42 (t, *J* = 7.2 Hz, 3H) ppm. ^{13}C NMR (100 MHz, CDCl$_3$) δ 166.1, 143.2, 130.6, 129.8, 128.8, 128.2, 106.6, 61.4, 14.5, 13.2 ppm.

4.1.2.14. tert-butyl 4-(2,5-dimethyl-1H-pyrrol-1-yl)benzoate (16). Yield: 94%. ^{1}H NMR (400 MHz, CDCl$_3$) δ 8.09 (d, *J* = 8.6 Hz, 2H), 7.26 (d, *J* = 8.6 Hz, 2H), 5.92 (s, 2H), 2.04 (s, 6H), 1.62 (s, 9H) ppm. ^{13}C NMR (100 MHz, CDCl$_3$) δ 142.8, 131.3, 130.5, 128.8, 128.1, 108.5, 81.6, 28.3, 13.2 ppm.

4.1.3. Synthesis of tert-butyl 2-(4-(2,5-dimethyl-1H-pyrrol-1-yl)phenoxy)acetate (12). To a stirred solution of 4-(2,5-dimethyl-1*H*-pyrrol-1-yl)phenol **8** (2.67 mmol) in acetone (10 mL), K$_2$CO$_3$ (8.0 mmol) was added and the resulting mixture was allowed to stir at room temperature for 30 minutes. After that, *tert*-butyl chloroacetate **10** (2.93 mmol) and sodium iodide (0.26 mmol) were added to the stirring solution and the reaction mixture was heated at 60 °C overnight. After evaporation of the solvent, the resulting crude was dissolved and extracted in ethyl acetate. The organic layer was washed with a saturated solution of NaHCO$_3$ and then with brine. The organic layer was subsequently collected, dried over MgSO$_4$, filtered, and concentrated in vacuo to give a crude that was purified by silica flash column chromatography (Hexane as eluent) to afford 395 mg of the pure product **12**. Yield: 50 %. ^{1}H NMR (400 MHz, CDCl$_3$) δ 7.14 (d, *J* = 8.7 Hz, 2H), 6.97 (d, *J* = 8.8 Hz, 2H), 5.89 (s, 2H), 4.58 (s, 2H), 2.02 (s, 6H), 1.52 (s, 9H) ppm. ^{13}C NMR (100 MHz, CDCl$_3$) δ 167.9, 157.3, 132.6, 129.3, 129.0, 115.0, 105.4, 82.5, 66.0, 28.1, 13.0 ppm.

4.1.4. General procedure for the synthesis of aldehydes **4**, **9** and **13**. Aldehydes were synthesized as described in the literature [18,19].

4.1.4.1. 1-cyclohexyl-2,5-dimethyl-1H-pyrrole-3-carbaldehyde (4a). Yield: 75%. ^{1}H NMR (400 MHz, CDCl$_3$) δ 9.19 (s, 1H), 5.65 (s, 1H), 3,40-3.38 (t, *J* = 3.7 Hz, 1H), 1.98 (s, 3H), 1.7 (s, 3H), 1.40-1.27 (m, 6H), 0.83-0.76 (m, 2H), 0.70-0.62 (m, 2H) ppm. ^{13}C NMR (100 MHz, CDCl$_3$) δ 184.4, 137.2, 129.4, 120.9, 107.0, 56.2, 31.3, 25.8, 24.8, 13.9, 11.2 ppm.

4.1.4.2. 2,5-dimethyl-1-(pyridin-2-yl)-1H-pyrrole-3-carbaldehyde (4b). (Used in the next step without further purification)

4.1.4.3. 1-(4-chlorobenzyl)-2,5-dimethyl-1H-pyrrole-3-carbaldehyde (4c). (Used in the next step without further purification)

*4.1.4.4. 2,5-dimethyl-1-(1-phenylethyl)-1H-pyrrole-3-carbaldehyde (**4d**)*. Yield: 73%. ^{1}H NMR (400 MHz, CDCl$_3$) δ 9.80 (s, 1H), 7.36-7.33 (m, 2H), 7.30-7.29 (m, 1H), 7.08-7.06 (m, 2H), 6.31 (s, 1H), 5.57-5.55 (d, *J* = 7.1 Hz, 1H), 2.18 (s, 3H), 2.05 (s, 3H), 1.90-1.88 (d, *J* = 7.2 Hz, 3H) ppm.

*4.1.4.5. 2,5-dimethyl-1-(pyridin-2-ylmethyl)-1H-pyrrole-3-carbaldehyde (**4e**)*. Yield: 26%. ^{1}H-NMR (400 MHz, CDCl$_3$) δ 9.85 (s, 1H), 7.63 (td, *J* = 7.7, 1.7 Hz, 2H), 7.21 (dd, *J* = 7.1, 5.3 Hz, 2H), 6.38 (s, 1H), 5.15 (s, 2H), 2.44 (s, 3H), 2.15 (s, 3H). ^{13}C NMR (100 MHz, CDCl$_3$) δ 185.2, 156.6, 149.9, 137.5, 130.2, 122.7, 122.1, 119.9, 106.7, 77.1, 48.8, 12.3, 10.6 ppm.

*4.1.4.6. 2,5-dimethyl-1-(4-methylbenzyl)-1H-pyrrole-3-carbaldehyde (**4f**)*. Yield: 16%. ^{1}H NMR (400 MHz, CDCl$_3$) δ 9.83 (s, 1H), 7.12 (d, *J* = 7.9 Hz, 2H), 6.79 (d, *J* = 8.0 Hz, 2H), 6.35 (s, 1H), 5.01 (s, 2H), 2.42 (s, 3H), 2.32 (s, 3H), 2.13 (s, 3H) ppm.

*4.1.4.7. 1-cyclopentyl-2,5-dimethyl-1H-pyrrole-3-carbaldehyde (**4g**)*. Yield: 61%. ^{1}H NMR (400 MHz, CDCl$_3$) δ 9.72 (s, 1H), 6.31 (s, 1H). 4.69-4.57 (m, 1H), 2.56 (3H), 2.29 (s, 3H), 2.14 – 2.06 (m, 4H), 1.98 – 1.92 (m, 4H) ppm.

*4.1.4.8. 1-(4-fluorobenzyl)-2,5-dimethyl-1H-pyrrole-3-carbaldehyde (**4h**)*. Yield 88%. ^{1}H NMR (400 MHz, CDCl$_3$) δ 9.84 (s, 1H), 7.01 (t, *J* = 8.7 Hz, 2H), 6.88-6.85 (m, 2H), 6.36 (br. s, 1H), 5.02 (s, 2H), 2.42 (s, 3H), 2.13 (s, 3H) ppm. ^{13}C NMR (100 MHz, CDCl$_3$) δ 185.3, 163.5, 161.1, 138.0, 132.3 (d), 130.2, 127.3, 127.2, 122.0, 116.2, 116.0, 106.7, 46.2, 12.3, 10.6 ppm.

*4.1.4.9. 1-(cyclohexylmethyl)-2,5-dimethyl-1H-pyrrole-3-carbaldehyde (**4i**)*. Yield: 34%. ^{1}H NMR (400 MHz, CDCl$_3$) δ 9.19 (s, 1H), 5.65 (s, 1H), 3.44 – 3.32 (m, 1H), 1.98 (s, 3H), 1.70 (s, 3H), 1.44 – 1.11 (m, 9H), 0.88 – 0.74 (m, 2H) ppm.

*4.1.4.10. 1-(benzo[d]thiazol-2-yl)-2,5-dimethyl-1H-pyrrole-3-carbaldehyde (**4j**)*. (Used in the next step without further purification)

*4.1.4.11. 1-(4-chlorophenyl)-2,5-dimethyl-1H-pyrrole-3-carbaldehyde (**4k**)*. Yield: 81%. ^{1}H NMR (400 MHz, CDCl$_3$) δ 9.84 (s, 1H), 7.30 (d, *J* = 8.5 Hz, 2H), 6.83 (d, *J* = 8.6 Hz, 2H), 6.37 (s, 1H), 5.02 (s, 2H), 2.41 (s, 3H), 2.12 (d, 3H) ppm.

*4.1.4.12. 1-(4-hydroxyphenyl)-2,5-dimethyl-1H-pyrrole-3-carbaldehyde (**9**)*. Yield: 39%. ^{1}H NMR (400 MHz, CD$_3$OD) δ 9.71 (s, 1H), 7.07 (d, *J* = 8.8 Hz, 2H), 6.93 (d, *J* = 8.9 Hz, 2H),

6.31 (br. s, 1H), 2.26 (s, 3H), 1.97 (s, 3H) ppm. ^{13}C NMR (100 MHz, CD$_3$OD) δ 187.2, 159.4, 133.2, 130.1, 129.5, 122.8, 117.2, 105.9, 12.6, 11.1 ppm.

4.1.4.13. 2-(4-(3-formyl-2,5-dimethyl-1H-pyrrol-1-yl)phenoxy)-N,N-dimethylacetamide (13). Yield: 40%. ^{1}H NMR (400 MHz, CDCl$_3$) δ 9.79 (s, 1H), 7.07-7.00 (m, 4H), 6.29 (s, 1H), 4.72 (s, 2H), 3.07 (s, 3H), 2.96 (s, 3H), 2.20 (s, 3H), 1.91 (s, 3H) ppm. ^{13}C NMR (100 MHz, CDCl$_3$) δ 185.1, 167.3, 158.3, 139.2, 131.3, 130.2, 129.0, 121.7, 115.5, 105.4, 67.3, 36.5, 35.7, 12.6, 11.2 ppm.

4.1.5. Synthesis of tert-butyl 2-(4-(3-formyl-2,5-dimethyl-1H-pyrrol-1-yl)phenoxy)acetate (11). To a stirred solution of 1-(4-hydroxyphenyl)-2,5-dimethyl-1*H*-pyrrole-3-carbaldehyde **9** (2.32 mmol) in dry DMF (5 mL), K$_2$CO$_3$ (4.64 mmol) was added and the resulting mixture was allowed to stir at room temperature for 30 minutes. After that, *tert*-butyl chloroacetate (3.48 mmol) and sodium iodide (0.26 mmol) were added to the stirring solution and the reaction mixture was heated at 90 °C overnight. After evaporation of the solvent, the resulting crude was dissolved and extracted in ethyl acetate. The organic layer was washed with a saturated solution of NaHCO$_3$ and then with brine. The organic layer was subsequently collected, dried over MgSO$_4$, filtered, and concentrated in vacuo. Removal of the solvent gave 750 mg of the desired product that proved to be pure enough to be used in the next step without any further purification. Yield: 98%. ^{1}H NMR (400 MHz, CDCl$_3$) δ 9.86 (s, 1H), 7.11 (d, J = 8.9 Hz, 2H), 7.00 (d, J = 8.9 Hz, 2H), 6.36 (br. s, 1H), 4.58 (s, 2H), 2.26 (s, 3H), 1.97 (s, 3H), 1.50 (s, 9H) ppm. ^{13}C NMR (100 MHz, CDCl$_3$) δ 185.4, 167.7, 131.4, 129.2, 115.6, 105.7, 82.9, 66.0, 28.2, 12.8, 11.4 ppm.

4.1.6. General procedure for the synthesis of aminoguanidines 7. Into a round bottom flask, the appropriate amine (3.06 mmol) and Et$_3$N (0.76 mmol) were dissolved in DCM (15 mL). Then a solution of 1,3-di-boc-2-trifluoromethylsulfonyl guanidine **6** (0.76 mmol) in DCM (15 mL) was added dropwise and the resulting mixture was stirred at room temperature for 24 h. After completion, the reaction mixture was concentrated under reduced pressure to give a crude residue that was purified with flash chromatography (EtOAc/MeOH 9:1 v/v), affording the desired aminoguanidine compounds **7**.

4.1.6.1. 1-(4-aminobutyl)-2,3-di-boc-guanidine (7a). Yield: 97 %. ^{1}H NMR (400 MHz, CDCl$_3$) δ 8.42 (br. s, 1H), 4.21 (br. s, 1H), 3.39 (t, J = 6.7 Hz, 2H), 2.86 (t, J = 6.7 Hz, 2H), 1.70-1.56 (m, 4H), 1.49 (d, J = 1.8 Hz, 18H) ppm. ^{13}C NMR (100 MHz, CDCl$_3$) δ 163.4, 156.4, 153.4, 83.4, 79.8, 40.8, 40.1, 28.4, 28.2, 26.2 ppm.

4.1.6.2. 1-(8-aminooctyl)-2,3-di-boc-guanidine (7b). Yield: 99 %. ^{1}H NMR (400 MHz, CD$_3$OD) δ 4.99 (br. s, 2H), 3.35 (t, *J* = 7.1 Hz, 2H), 2.77 (t, *J* = 7.5 Hz, 2H), 1.63-1.55 (m, 4H), 1.53 (s, 9H), 1.47 (s, 9H), 1.37 (br. s, 8H) ppm. ^{13}C NMR (100 MHz, CD$_3$OD) δ 164.5, 157.4, 154.2, 84.4, 80.2, 41.7, 41.6, 31.1, 30.2, 30.1, 30.0, 28.6, 28.3, 27.7, 27.6 ppm.

4.1.6.3. 1-(4-aminocyclohexyl)-2,3-di-boc-guanidine (7c). Yield: 94 %. ^{1}H NMR (400 MHz, CDCl$_3$) δ 11.49 (br. s, 1H), 8.19 (d, *J* = 8.2 Hz, 1H), 4.01-3.91 (m, 1H), 2.73-2.62 (m, 2H), 2.07-2.03 (m, 2H), 1.92-1.88 (m, 2H), 1.48 (d, J = 6.4 Hz, 18H), 1.30-1.20 (m, 4H) ppm. ^{13}C NMR (100 MHz, CDCl$_3$) δ 163.9, 155.6, 153.4, 83.1, 79.3, 50.0, 48.4, 34.5, 31.6, 28.4, 28.2 ppm.

4.1.7. General procedure for the synthesis of pyrroles 5. Pyrroles 5 were synthesized as previously described in the literature [18,19].

(i) General procedure for boc-deprotection and tert-butyl ester-cleavage. Into a sealed vial, 3 mL of a freshly prepared HCl/AcOEt solution was added to the appropriate Boc-protected pyrrole or *tert*-butyl ester derivative (0.2 mmol). The resulting mixture was stirred at room temperature for 24 h and then the solvent was removed under reduced pressure. The residue was washed several times with small portions of cold Et$_2$O affording the desired compounds as HCl salts in quantitative yields.

4.1.7.1. 1-cyclohexyl-N-((1-cyclohexyl-2,5-dimethyl-1H-pyrrol-3-yl)methyl)methanamine (5a). Yield: 13%. ^{1}H NMR (400 MHz, CDCl$_3$) δ 5.91 (s, 1H), 3.87 (s, 1H), 3.78 (s, 2H), 2.58-2.56 (d, *J* = 8 Hz, 2H), 2.25-2.24 (d, *J* = 4 Hz, 6H), 1.91-1.81 (m, 8H), 1.73-1.68 (m, 6H), 1.40-1.34 (m, 2H), 1.20-1.10 (m, 2H), 0.97-0.86 (m, 4H) ppm. ^{13}C NMR (100 MHz, CDCl$_3$) δ 128.6, 127.8, 127.0, 108.5, 56.7, 52.6, 44.0, 35.6, 32.4, 31.1, 26.6, 26.3, 25.8, 25.7, 14.8, 11.8 ppm. HRMS: m/z (ESI) calculated for C$_{20}$H$_{35}$N$_2$$^+$ 303.2795, found: 303.2801 [M + H]$^+$.

4.1.7.2. 1-cyclohexyl-N-((2,5-dimethyl-1-(pyridin-2-yl)-1H-pyrrol-3-yl)methyl)methanamine (5b). Yield: 55%. ^{1}H NMR (400 MHz, CDCl$_3$) δ 8.53-8.51 (m, 1H), 7.76-7.72 (m, 1H), 7.23-7.20 (m, 1H), 7.13-7.11 (d, *J* = 7.9 Hz, 1H), 5.86 (s, 1H), 3.52 (s, 2H), 2.44-2.42 (d, *J* = 6.7 Hz, 2H), 2.26 (s, 1H), 2.02 (s, 3H), 1.99 (s, 3H), 1.66-1.62 (m, 6H), 0.92-0.79 (m, 5H) ppm. ^{13}C NMR (100 MHz, CDCl$_3$) δ 152.9, 149.0, 145.1, 135.5, 127.8, 127.0, 117.9, 116.5, 108.4, 56.8, 44.1, 35.7, 31.2, 26.3, 25.7, 14.5, 11.7 ppm. HRMS: m/z (ESI) calcd for C$_{19}$H$_{28}$N$_3$$^+$ 298.2278, found: 298.2276 [M + H]$^+$.

*4.1.7.3. N-benzyl-1-(2,5-dimethyl-1-(pyridin-2-yl)-1H-pyrrol-3-yl)methanamine (5c).*Yield: 45%. ^{1}H NMR (400 MHz, CDCl$_3$) δ 8.58-8.56 (dd, J = 4.9, 1.3 Hz, 1H), 7.80-7.76 (td, J = 7.7, 1.9 Hz, 1H), 7.35-7.33 (m, 2H), 7.31 (s, 1H), 7.29 (s, 1H), 7.26-7.24 (m, 1H), 7.23-7.20 (m, 1H), 7.18-7.16 (ddd, J = 7.6 Hz, 3.1, 1.8, 1H), 5.94 (s, 1H), 3.83 (s, 2H), 3.62 (s, 2H), 2.08 (s, 3H), 2.02 (s, 3H), 1.22 (s, 1H). ^{13}C NMR (100 MHz, CDCl$_3$) δ 152.1, 149.4, 140.7, 137.9, 128.3, 128.2, 127.9, 126.8, 125.5, 122.3, 122.1, 118.6, 108.1, 53.2, 44.8, 13.0, 10.8 ppm. HRMS: m/z (ESI) calcd for C$_{19}$H$_{22}$N$_3$$^+$ 292.1808, found: 292.1812 [M + H]$^+$.

4.1.7.4.   N-benzyl-1-(1-(4-chlorobenzyl)-2,5-dimethyl-1H-pyrrol-3-yl)methanamine   (5d). Yield: 60%. ^{1}H NMR (400 MHz, CDCl$_3$) δ 7.34-7.29 (m, 4H), 7.23-7.21 (m, 3H), 6.78-6.76 (d, J = 8.3 Hz, 2H), 5.88 (s, 1H), 4.91 (s, 2H), 3.8 (s, 2H), 3.6 (s, 2H), 2.09 (s, 3H), 2.01 (s, 3H) ppm. ^{13}C NMR (100 MHz, CDCl$_3$) δ 140.7, 137.2, 132.9, 128.9, 128.4, 128.3, 127.1, 127.1, 126.8, 124.9, 117.7, 106.8, 53.3, 46.3, 45.0, 12.3, 10.0 ppm. HRMS: m/z (ESI) calcd for C$_{21}$H$_{24}$ClN$_2$$^+$ 339.1623, found: 339.1627 [M + H]$^+$.

4.1.7.5.   1-(1-(4-chlorobenzyl)-2,5-dimethyl-1H-pyrrol-3-yl)-N-(cyclohexylmethyl)methanamine (5e). Yield: 68%. ^{1}H NMR (400 MHz, CDCl$_3$) δ 7.17-7.15 (d, J = 8.4 Hz, 2H), 6.72-6.7 (d, J = 8.3 Hz, 2H), 5.81 (s, 1H), 4.86 (s, 2H), 3.49 (s, 2H), 2.40-2.39 (d, J = 6.7 Hz, 2H), 2.02 (s, 3H), 1.98 (s, 3H), 1.69-1.61 (m, 4H), 1.42 (m, 1H), 1.12 (m, 4H), 0.84 (m, 2H) ppm. ^{13}C NMR (100 MHz, CDCl$_3$) δ 137.5, 133.2, 129.2, 127.4, 125.0, 118.4, 107.1, 56.7, 46.6, 46.3, 38.3, 32.0, 27.1, 26.5, 12.6, 10.3 ppm. HRMS: m/z (ESI) calcd for C$_{21}$H$_{30}$ClN$_2$$^+$ 345.2092, found: 345.2099 [M + H]$^+$.

4.1.7.6. N-benzyl-1-(2,5-dimethyl-1-(1-phenylethyl)-1H-pyrrol-3-yl)methanamine (5f). Yield: 60%. ^{1}H NMR (400 MHz, CDCl$_3$) δ 7.36-7.32 (m, 3H), 7.31-7.28 (m, 3H), 7.25-7.21 (m, 2H), 7.05-7.02 (m, 2H), 6.85 (s, 1H), 5.49-5.43 (q, J = 7.2 Hz, 1H), 3.82 (s, 2H), 3.6 (s, 2H), 2.07 (s, 3H), 1.98 (s, 3H), 1.86-1.84 (d, J = 7.2 Hz, 3H) ppm. ^{13}C NMR (100 MHz, CDCl$_3$) δ 142.6, 140.7, 128.5, 128.4, 128.3, 127.5, 126.9, 126.8, 126.1, 125.3, 117.6, 107.4, 53.3, 52.6, 45.1, 19.5, 13.8, 11.2 ppm. HRMS: m/z (ESI+) calcd for C$_{22}$H$_{27}$N$_2$$^+$ 319.2169, found: 319.2173 [M + H]$^+$.

4.1.7.7. 1-cyclohexyl-N-((2,5-dimethyl-1-(1-phenylethyl)-1H-pyrrol-3-yl)methyl)methanamine (5g). Yield: 64%. ^{1}H NMR (400 MHz, CDCl$_3$) δ 7.31-7.28 (m, 2H), 7.25- 7.23 (d, J = 7.4 Hz, 1H), 7.04-7.01 (m, 2H), 5.85 (s, 1H), 5.46-5.44 (d, J = 8 Hz, 1H), 3.58 (s, 2H), 3.1-3.07 (m, 1H), 2.49-2.47 (d, J = 6.7 Hz, 2H), 2.05 (s, 3H), 2.02 (s, 3H), 1.86-1.84 (d, J = 7.2 Hz, 3H), 1.78-1.69 (m, 5H), 1.19-1.13 (m, 2H), 0.96-0.83 (m, 4H) ppm. ^{13}C NMR (100 MHz, CDCl$_3$) δ

142.6, 128.5, 127.5, 126.9, 126.1, 125.3, 116.4, 107.5, 77.3, 52.6, 46.0, 38.0, 30.9, 26.1, 25.9, 19.5, 13.8, 11.2 ppm. HRMS: m/z (ESI) calcd for $C_{22}H_{33}N_2^+$ 325.3628, found: 325.3628 [M + H]$^+$.

4.1.7.8. 1-cyclohexyl-N-((2,5-dimethyl-1-(pyridin-2-ylmethyl)-1H-pyrrol-3-yl)methyl)methanamine (5h). Yield: 62%. ^{1}H NMR (400 MHz, CDCl$_3$) δ 8.57-8.55 (m, 1H), 7.60-7.56 (m, 1H), 7.18-7.15 (dd, *J* = 7.4 Hz, 1H), 6.44-6.42 (d, *J* = 7.9 Hz, 1H), 6.10 (s, 1H), 5.09 (s, 2H), 3.88 (s, 2H), 2.61-2.60 (d, *J* = 6.9 Hz, 2H), 2.11 (s, 3H), 2.07 (s, 3H), 2.04-1.98 (m, 2H), 1.89-1.86 (m, 2H), 1.74-1.70 (m, 3H), 1.26-1.24 (m, 2H), 0.97-0.94 (m, 2H). ^{13}C NMR (100 MHz CDCl$_3$) δ 158.0, 149.4, 137.3, 128.3, 127.5, 122.2, 119.8, 107.8, 51.8, 50.0, 43.5, 35.2, 31.0, 26.1, 25.5, 12.1, 10.1 ppm. HRMS: m/z (ESI) calcd for $C_{20}H_{30}N_3^+$ 312.2434, found: 312.2439 [M + H]$^+$.

4.1.7.9. N-benzyl-1-(2,5-dimethyl-1-(p-tolyl)-1H-pyrrol-3-yl)methanamine (5i). Yield: 56%. ^{1}H NMR (400 MHz, CDCl$_3$) δ 7.39-7.37 (m, 2H), 7.34-7.30 (m, 3H), 7.10-7.08 (d, *J* = 7.8 Hz, 2H), 6.78-6.76 (d, *J* = 8.0 Hz, 2H), 5.94 (s, 1H), 3.85 (s, 2H), 3.65 (s, 2H), 2.31 (s, 3H), 2.12 (s, 3H), 2.01 (s, 3H) ppm. ^{13}C NMR (100 MHz, CDCl$_3$) δ 136.8, 135.5, 133.4, 129.5, 128.9, 128.7, 128.5, 128.0, 127.6, 127.3, 125.7, 106.7, 46.7, 44.42, 21.2, 12.4, 10.1 ppm. HRMS: m/z (ESI) calcd for $C_{21}H_{25}N_2^+$ 305.2012, found: 305.2013 [M + H]$^+$.

4.1.7.10. 1-cyclohexyl-N-((2,5-dimethyl-1-(p-tolyl)-1H-pyrrol-3-yl)methyl)methanamine (5j). Yield: 89%. ^{1}H NMR (400 MHz, CDCl$_3$) δ 7.09-7.07 (d, *J* = 7.8 Hz, 2H), 6.77-6.75 (d, *J* = 8.1 Hz, 2H), 5.91 (br s, 1H), 3.63 (br s, 2H), 2.50-2.49 (d, *J* = 6.5 Hz, 2H), 2.31 (s, 3H), 2.11 (s, 3H), 2.08 (s, 3H), 1.98 (s, 1H), 1.82-1.80 (m, 1H), 1.72-1.69 (m, 5H), 1.26-1.23 (m, 3H), 0.93-0.90 (m, 2H). ^{13}C NMR (100 MHz, CDCl$_3$) δ 140.0, 135.5, 134.1, 129.6, 129.5, 127.5, 125.7, 106.9, 77.1, 46.7, 31.6, 30.9, 26.2, 26.1, 21.1, 12.3, 10.1 ppm. HRMS: m/z (ESI) calcd for $C_{21}H_{31}N_2^+$ 311.2482, found: 311.2486 [M + H]$^+$.

4.1.7.11. N-benzyl-1-(1-cyclopentyl-2,5-dimethyl-1H-pyrrol-3-yl)methanamine (5k). Yield: 95%. ^{1}H NMR (400 MHz, CDCl$_3$) δ 7.38-7.36 (m, 2H), 7.35-7.30 (m, 3H), 5.83 (s, 1H), 4.52-4.43 (m, 1H), 3.84 (s, 2H), 3.58 (s, 2H), 2.25 (s, 3H), 2.18 (s, 3H), 2.05-1.84 (m, 7H), 1.70-1.62 (m, 2H) ppm. ^{13}C NMR (100 MHz, CDCl$_3$) δ 139.8, 128.9, 128.7, 128.5, 127.2, 127.1, 126.9, 107.5, 56.5, 52.9, 44.8, 31.4, 25.2, 14.1, 11.5 ppm. HRMS: m/z (ESI) calcd for $C_{19}H_{27}N_2^+$ 283.2169, found: 283.2170 [M + H]$^+$.

4.1.7.12.   1-cyclohexyl-N-((1-cyclopentyl-2,5-dimethyl-1H-pyrrol-3-yl)methyl)methanamine (5l). Yield: 82%. ^{1}H NMR (400 MHz, CDCl$_3$) δ 5.84 (s, 1H), 4.52-4.47 (m, 1H), 3.62-3.61 (m, 2H), 2.52-2.51 (d, J = 6.3 Hz, 2H), 2.25-2.24 (m, 5H), 2.02-1.96 (m, 2H), 1.95-1.85 (m, 3H), 1.82-1.78 (m, 2H), 1.72-1.63 (m, 5H), 1.29-1.11 (m, 6H), 0.96-0.87 (m, 3H) ppm. ^{13}C NMR (100 MHz, CDCl$_3$) δ 128.6, 127.4, 126.0, 107.9, 56.3, 44.7, 37.8, 36.5, 31.2, 31.2, 26.4, 25.8, 25.0, 13.9, 11.3 ppm. HRMS: m/z (ESI) calcd for C$_{19}$H$_{33}$N$_2^+$ 289.2638, found: 289.2637 [M + H]$^+$.

4.1.7.13.   N-benzyl-1-(1-(4-fluorobenzyl)-2,5-dimethyl-1H-pyrrol-3-yl)methanamine (5m). Yield: 77%. ^{1}H NMR (400 MHz, CDCl$_3$) δ 7.37-7.30 (m, 5H), 7.00-6.95 (m, 2H), 6.85-6.81 (dd, J = 8.7, 5.3, 2H), 5.93 (s, 1H), 4.95 (s, 2H), 3.84 (s, 2H), 3.63 (s, 2H), 2.12 (s, 3H), 2.03 (s, 3H), 1.26 (s, 1H) ppm. ^{13}C NMR (100 MHz, CDCl$_3$) δ 162.9, 134.0, 128.4, 128.2, 128.2, 127.0, 127.0, 126.8, 124.9, 115.5, 115.3, 106.6, 52.6, 46.0, 44.4, 12.0, 10.0 ppm. HRMS: m/z (ESI+) calcd for C$_{21}$H$_{24}$FN$_2^+$ 323.1918, found: 323.1918 [M + H]$^+$.

4.1.7.14.   1-cyclohexyl-N-((1-(4-fluorobenzyl)-2,5-dimethyl-1H-pyrrol-3-yl)methyl)methanamine (5n). Yield: 94% ^{1}H NMR (400 MHz CDCl$_3$) δ 7.00-6.94 (m, 2H), 6.84-6.80 (m, 2H), 5.93 (s, 1H), 4.95 (s, 2H), 3.64 (s, 2H), 2.50-2.49 (d, J = 6.7 Hz, 2H), 2.11 (s, 3H), 2.08 (s, 3H), 1.80-1.76 (m, 2H), 1.73-1.68 (m, 3H), 1.58-1.53 (m, 1H), 1.27-1.15 (m, 3H), 0.96-0.86 (m, 2H) ppm. ^{13}C NMR (100 MHz, CDCl$_3$) δ 162.7, 133.7, 127.0, 126.7, 125.3, 115.3, 115.1, 106.7, 54.2, 45.8, 44.5, 36.5, 31.0, 26.1, 25.5, 11.8, 9.6 ppm. HRMS: m/z (ESI) calcd for C$_{21}$H$_{30}$FN$_2^+$ 329.2388, found: 329.2393 [M + H]$^+$.

4.1.7.15.   N-benzyl-1-(1-(cyclohexylmethyl)-2,5-dimethyl-1H-pyrrol-3-yl)methanamine (5o). Yield: 93% ^{1}H NMR (400 MHz, CDCl$_3$) δ 7.38-7.31 (m, 5H), 5.83 (s, 1H), 3.88-3.83 (m, 2H), 3.61 (s, 2H), 3.52 (d, J = 6.9 Hz, 2H), 2.17 (s, 3H), 2.11 (s, 3H), 1.74-1.67 (m, 3H), 1.64-1.61 (m, 2H), 1.27-1.27 (m, 2H), 1.18-1.16 (m, 2H), 0.99-0.85 (m, 3H) ppm. ^{13}C NMR (100 MHz, CDCl$_3$) δ 140.0, 128.6, 128.4, 127.3, 127.2, 127.0, 126.9, 106.2, 50.2, 46.6, 44.8, 39.6, 31.1, 26.5, 26.1, 12.8, 10.5 ppm. HRMS: m/z (ESI) calcd for C$_{21}$H$_{31}$N$_2^+$ 311.2482, found: 311.2435 [M + H]$^+$.

4.1.7.16.   1-(1-(benzo[d]thiazol-2-yl)-2,5-dimethyl-1H-pyrrol-3-yl)-N-benzylmethanamine (5p). Yield: 94% ^{1}H NMR (400 MHz, CDCl$_3$) δ 8.04 (d, J = 8.1 Hz, 1H), 7.87 (d, J = 8.0 Hz, 1H), 7.53 (ddd, J = 8.2, 7.3, 1.3 Hz, 1H), 7.47 – 7.42 (m, 1H), 7.39 (d, J = 7.0 Hz, 2H), 7.36 – 7.31 (m, 3H), 6.05 (s, 1H), 5.30 (s, 1H), 3.86 (s, 2H), 3.65 (s, 2H), 2.28 (s, 3H), 2.21 (s, 3H) ppm. ^{13}C NMR (100 MHz, CDCl$_3$) δ 158.5, 150.3, 140.3, 135.1, 129.3, 128.3, 128.1, 126.8,

126.8, 126.4, 125.5, 123.4, 121.4, 120.0, 109.8, 53.0, 44.5, 13.3, 11.0 ppm. HRMS: m/z (ESI) calcd for $C_{21}H_{22}N_3S^+$ 348.1529, found: 348.1544 [M + H]$^+$.

4.1.7.17. *1-(1-(benzo[d]thiazol-2-yl)-2,5-dimethyl-1H-pyrrol-3-yl)-N-(cyclohexylmethyl)methanamine (5q)*. Yield: 60% ^{1}H NMR (400 MHz, CDCl$_3$) δ 8.05-8.03 (d, *J* = 8.1 Hz, 1H), 7.89-7.87 (d, *J* = 8.1 Hz, 1H), 7.56-7.52 (m, 1H), 7.47-7.43 (m, 1H), 6.07 (s, 1H), 3.67 (s, 2H), 2.54-2.52 (d, 8 Hz, 2H), 2.29 (s, 3H), 2.27 (s, 3H), 1.83-1.79 (m, 2H), 1.76-1.70 (m, 3H), 1.66 (br s, 1H), 1.29-1.17 (m, 3H), 0.99-0.90 (m, 2H) ppm. ^{13}C NMR (100 MHz, CDCl$_3$) δ 158.2, 150.0, 134.8, 129.1, 126.7, 126.2, 125.2, 123.1, 121.1, 109.6, 55.2, 44.8, 37.2, 31.1, 26.3, 25.7, 13.0, 10.7 ppm. HRMS: m/z (ESI) calcd for $C_{21}H_{28}N_3S^+$ 354.1998, found: 354.1996 [M + H]$^+$.

4.1.7.18. *N′-((1-(4-chlorophenyl)-2,5-dimethyl-1H-pyrrol-3-yl)methyl)isonicotinohydrazide (5r)*. Yield: 59%. ^{1}H NMR (400 MHz, CDCl$_3$) δ 8.75 (m, 2H), 7.82 (m, 2H), 7.47 (d, *J* = 8.1 Hz, 2H), 7.17-7.11 (m, 2H), 6.44 (s, 1H), 2.12 (s, 2H), 1.98 (s, 3H), 1.25 (s, 3H) ppm. ^{13}C NMR (100 MHz, CDCl$_3$) δ 167.3, 149.7, 136.3, 134.7, 132.0, 130.4, 129.9, 129.5, 128.1, 124.0, 121.2, 105.3, 48.6, 12.9, 11.4 ppm. HRMS: m/z (ESI) calculated for $C_{19}H_{20}ClN_4O^+$ 355.1320, found: 709.5138 [2M + H]$^+$.

4.1.7.19. *2-(4-(3-((cyclohexylamino)methyl)-2,5-dimethyl-1H-pyrrol-1-yl)phenoxy)-N,N-dimethylacetamide (5s)*. Yield: 59 %. ^{1}H NMR (400 MHz, CDCl$_3$) δ 7.07 (d, *J* = 8.8 Hz, 2H), 6.99 (d, *J* = 8.9 Hz, 2H), 5.94 (s, 1H), 4.72 (s, 2H), 3.69 (s, 2H), 3.11 (s, 3H), 3.00 (s, 3H), 2.67-2.60 (m, 1H), 2.01-1.97 (m, 2H), 1.95 (s, 3H), 1.94 (s, 3H), 1.80-1.70 (m, 2H), 1.63-1.58 (m, 1H), 1.27-1.22 (m, 5H) ppm. ^{13}C NMR (100 MHz, CDCl$_3$) δ 167.7, 157.5, 132.6, 129.5, 128.5, 126.6, 115.1, 106.7, 67.7, 55.9, 41.9, 36.7, 35.8, 32.4, 26.0, 25.1, 12.9, 10.8 ppm. HRMS: m/z (ESI) calculated for $C_{23}H_{34}N_3O_2^+$ 384.2646, found: 384.2634 [M + H]$^+$.

4.1.7.20. boc-protected 2-(4-(3-(((8-guanidinooctyl)amino)methyl)-2,5-dimethyl-1H-pyrrol-1-yl)phenoxy)-N,N-dimethylacetamide (5t intermediate). Yield: 63 %. ^{1}H NMR (400 MHz, CDCl$_3$) δ 11.49 (br. s, 1H), 8.27 (s, 1H), 7.07 (d, *J* = 8.8 Hz, 2H), 6.98 (d, *J* = 8.9 Hz, 2H), 5.98 (s, 1H), 4.71 (s, 2H), 3.70 (s, 2H), 3.40-3.35 (m, 4H), 3.10 (s, 3H), 2.99 (s, 3H), 2.73-2.64 (m, 4H), 1.95 (s, 6H), 1.63 (br. s, 2H), 1.53 (br. s, 2H), 1.48 (s, 9H), 1.47 (s, 9H), 1.40 (br. s, 1H), 1.29 (br. s, 9H) ppm. ^{13}C NMR (100 MHz, CDCl$_3$) δ 167.6, 163.7, 157.5, 156.2, 153.4, 132.5, 129.5, 128.7, 127.1, 115.2, 106.9, 83.1, 79.3, 67.7, 48.2, 44.8, 42.2, 41.0, 36.7, 35.8, 33.7, 29.4, 29.3, 29.0, 28.4, 28.2, 27.3, 26.9, 12.9, 10.9 ppm.

4.1.7.21.   2-(4-(3-(((8-guanidinooctyl)amino)methyl)-2,5-dimethyl-1H-pyrrol-1-yl)phenoxy)-N,N-dimethylacetamide (5t). Yield: 100 %. ^{1}H NMR (400 MHz, DMSO-d$_6$) δ 10.36 (br. s, 1H), 8.94 (br. s, 1H), 8.07-7.90 (m, 2H), 7.60-7.02 (m, 4H), 6.75 (br. s, 1H), 4.88 (br. s, 2H), 4.10-3.80 (m, 4H), 3.15-3.01 (m, 4H), 2.85 (s, 3H), 2.73 (s, 3H), 2.06-1.92 (m, 3H), 1.83- 1.45 (m, 6H), 1.28 (br. s, 7H) ppm. ^{13}C NMR (100 MHz, DMSO-d$_6$) δ 166.9, 156.9, 143.9, 129.0, 128.8, 128.5, 128.2, 127.0, 124.2, 115.4, 65.8, 48.5, 47.4, 41.7, 40.5, 35.5, 34.9, 28.3, 28.3, 25.8, 25.6, 12.6, 10.6 ppm. HRMS: m/z (ESI) calculated for C$_{26}$H$_{43}$N$_6$O$_2$$^+$ 471.3442, found: 471.3401 [M + H]$^+$.

4.1.7.22.   boc-protected   1-(4-(((1-(4-chlorophenyl)-2,5-dimethyl-1H-pyrrol-3-yl)methyl)amino)cyclohexyl)guanidine (5u intermediate). Yield: 79%. ^{1}H NMR (400 MHz, CDCl$_3$) δ 11.53 (br. s, 1H), 8.20 (d, *J* = 8.2 Hz, 1H), 7.43 (d, *J* = 8.6 Hz, 2H), 7.12 (d, *J* = 8.6 Hz, 2H), 6.00 (s, 1H), 4.07-3.98 (m, 1H), 3.70 (s, 2H), 2.69-2.61 (m, 1H), 2.15-2.08 (m, 4H), 1.99 (s, 3H), 1.50 (s, 9H), 1.49 (s, 9H), 1.29-1.22 (m, 4H) ppm. ^{13}C NMR (100 MHz, CDCl$_3$) δ 164.0, 155.5, 153.5, 137.5, 133.7, 129.7, 129.5, 128.4, 107.4, 83.1, 79.3, 60.5, 48.6, 31.5, 28.4, 28.2, 12.9, 10.9 ppm.

4.1.7.23.   1-(4-(((1-(4-chlorophenyl)-2,5-dimethyl-1H-pyrrol-3-yl)methyl)amino)cyclohexyl)guanidine (5u). Yield: 100 %. ^{1}H NMR (400 MHz, CDCl$_3$) δ 10.56 (br. s, 1H), 9.20 (br. s, 1H), 7.42 (d, J = 8.5 Hz, 2H), 7.11 (d, *J* = 8.5 Hz, 2H), 6.22 (s, 1H), 3.99 (br. s, 2H), 3.02 (br. s, 1H), 2.30-2.25 (m, 3H), 2.15 (br. s, 1H), 2.00 (s, 3H), 1.94 (s, 3H), 1.45-1.24 (m, 5H) ppm. ^{13}C NMR (100 MHz, CDCl$_3$) δ 156.8, 152.6, 136.8, 134.2, 129.7, 128.9, 110.0, 52.7, 49.6, 40.5, 29.7, 12.9, 11.3 ppm. HRMS: m/z (ESI) calculated for C$_{20}$H$_{29}$ClN$_5$$^+$ 374.2106, found: 374.2093 [M + H]$^+$.

4.1.7.24. boc-protected tert-butyl 2-(4-(3-(((8-guanidinooctyl)amino)methyl)-2,5-dimethyl-1H-pyrrol-1-yl)phenoxy)acetate (5v intermediate).Yield: 59 %. ^{1}H NMR (400 MHz, CDCl$_3$) δ 11.49 (br. s, 1H), 8.28 (br. s, 1H), 7.08 (d, *J* = 8.8 Hz, 2H), 6.93 (d, *J* = 8.8 Hz, 2H), 5.89 (s, 1H), 4.54 (s, 2H), 3.58 (s, 2H), 3.41-3.36 (m, 2H), 2.65 (t, *J* = 7.2 Hz, 2H), 1.96 (s, 3H), 1.94 (s, 3H), 1.56-1.52 (m, 2H), 1.49 (s, 9H), 1.48 (s, 9H), 1.32-1.26 (m, 9H) ppm. ^{13}C NMR (100 MHz, CDCl$_3$) δ 167.9, 163.7, 157.3, 156.2, 153.4, 132.7, 129.4, 128.2, 125.8, 117.7, 115.0, 106.5, 83.0, 82.6, 79.2, 66.0, 49.8, 45.9, 41.1, 30.1, 29.5, 29.3, 29.0, 28.4, 28.2, 28.1, 27.5, 26.9, 12.8, 10.7 ppm.

4.1.7.25.   2-(4-(3-(((8-guanidinooctyl)amino)methyl)-2,5-dimethyl-1H-pyrrol-1-yl)phenoxy)acetic acid (5v). Yield: 100 %. ^{1}H NMR (400 MHz, CD$_3$OD) δ 7.13-7.06 (m, 4H),

6.00 (br. s, 1H), 4.74 (s, 2H), 4.27 (q, J = 7.2 Hz, 1H), 4.02 (s, 2H), 3.17 (t, J = 7.2 Hz, 2H), 3.00 (t, J = 8.0 Hz, 2H), 2.00 (s, 3H), 1.97 (s, 3H), 1.75-1.68 (m, 2H), 1.60-1.57 (m, 2H), 1.43-1.38 (m, 10H) ppm. ^{13}C NMR (100 MHz, CD$_3$OD) δ 172.5, 159.4, 158.8, 133.2, 130.8, 130.6, 130.3, 116.5, 109.8, 66.3, 66.2, 47.8, 45.0, 42.6, 30.3, 30.2, 30.0, 28.3, 27.8, 27.7, 27.3, 12.9, 10.9 ppm. HRMS: m/z (ESI) calculated for C$_{24}$H$_{36}$N$_5$O$_3$$^-$ 442.2824, found: 442.2792 [M - H]$^-$.

4.1.7.26. boc-protected 1-(4-(((1-(4-chlorophenyl)-2,5-dimethyl-1H-pyrrol-3-yl)methyl)amino)butyl)guanidine (5w intermediate). Yield: 56 %. ^{1}H NMR (400 MHz, CDCl$_3$) δ 11.49 (br. s, 1H), 8.33 (br. s, 1H), 7.41 (d, J = 8.6 Hz, 2H), 7.12 (d, J = 8.5 Hz, 2H), 5.91 (br. s, 1H), 3.59 (s, 2H), 3.45-3.40 (m, 2H), 2.69 (t, J = 6.5 Hz, 2H), 1.99 (s, 3H), 1.96 (s, 3H), 1.66-1.58 (m, 4H), 1.49 (s, 9H), 1.48 (s, 9H) ppm. ^{13}C NMR (100 MHz, CDCl$_3$) δ 163.8, 156.2, 153.4, 137.7, 133.6, 129.7, 129.4, 128.1, 125.7, 118.1, 107.2, 83.1, 79.3, 49.2, 45.7, 40.9, 28.4, 28.2, 27.5, 27.1, 12.9, 10.8 ppm.

4.1.7.27. 1-(4-(((1-(4-chlorophenyl)-2,5-dimethyl-1H-pyrrol-3-yl)methyl)amino)butyl)guanidine (5w). Yield: 100 %. ^{1}H NMR (400 MHz, CD$_3$OD) δ 7.50 (d, J = 8.4 Hz, 2H), 7.18 (d, J = 8.4 Hz, 2H), 5.45 (s, 1H), 4.01 (s, 2H), 3.57 (d, J = 7.1 Hz, 2H), 3.22 (t, J = 6.8 Hz, 2H), 2.00 (s, 3H), 1.95 (s, 3H), 1.69- 1.65 (2H), 1.14 (t, J = 7.0 Hz, 2H) ppm. ^{13}C NMR (100 MHz, CD$_3$OD) δ 158.8, 138.5, 135.5, 131.5, 131.1, 130.8, 130.6, 130.1, 126.1, 110.4, 47.3, 45.0, 42.0, 28.6, 27.2, 12.8, 10.9 ppm. HRMS: m/z (ESI) calculated for C$_{18}$H$_{27}$ClN$_5$$^+$ 348.1950, found: 348.2003 [M + H]$^+$.

4.1.7.28. boc-protected 1-(8-(((1-(4-chlorophenyl)-2,5-dimethyl-1H-pyrrol-3-yl)methyl)amino)octyl)guanidine (5x intermediate). Yield: 25 %. ^{1}H NMR (400 MHz, CDCl$_3$) δ 11.48 (br. s, 1H), 8.27 (br. s, 1H), 7.41 (d, J = 8.6 Hz, 2H), 7.09 (d, J = 8.5 Hz, 2H), 6.18 (s, 1H), 3.91 (s, 2H), 3.39-3.34 (m, 2H), 2.85- 2.81 (m, 2H), 2.01 (s, 3H), 1.95 (s, 3H), 1.85 (br. s, 2H), 1.57-1.52 (m, 2H), 1.49 (s, 9H), 1.48 (s, 9H), 1.32-1.27 (m, 8H) ppm. ^{13}C NMR (100 MHz, CDCl$_3$) δ 163.8, 156.2, 153.4, 137.0, 134.1, 129.7, 129.6, 129.2, 128.9, 109.1, 108.3, 83.1, 79.3, 45.6, 42.9, 41.0, 29.8, 29.3, 29.1, 29.0, 28.4, 28.2, 27.0, 26.9, 12.8, 11.1 ppm.

4.1.7.29. 1-(8-(((1-(4-chlorophenyl)-2,5-dimethyl-1H-pyrrol-3-yl)methyl)amino)octyl)guanidine (5x). Yield: 100 %. ^{1}H NMR (400 MHz, CD$_3$OD) δ 7.55 (d, J = 8.6 Hz, 2H), 7.21 (d, J = 8.6 Hz, 2H), 6.05 (s, 1H), 4.03 (s, 2H), 3.16 (t, J = 7.0 Hz, 2H), 3.01 (t, J = 7.9 Hz, 2H), 2.03 (s, 3H), 2.00 (s, 3H), 1.75-1.69 (m, 2H), 1.63-1.57 (m, 2H), 1.44-1.39 (m, 8H) ppm. ^{13}C NMR (100 MHz, CD$_3$OD) δ 158.8, 138.5, 135.5, 131.5, 130.9, 130.6,

130.1, 110.5, 47.9, 44.9, 42.6, 30.3, 30.2, 30.0, 27.8, 27.7, 27.3, 12.8, 10.9 ppm. HRMS: m/z (ESI) calculated for $C_{22}H_{35}ClN_5^+$ 404.2576, found: 404.2593 $[M + H]^+$.

4.1.7.30.   tert-butyl   2-(4-(3-((cyclohexylamino)methyl)-2,5-dimethyl-1H-pyrrol-1-yl)phenoxy)acetate (5y intermediate). Yield: 69 %. ^{1}H NMR (400 MHz, CDCl3) δ 7.09 (d, *J* = 8.7 Hz, 2H), 6.94 (d, *J* = 8.7 Hz, 2H), 5.90 (s, 1H), 4.55 (s, 2H), 3.62 (s, 2H), 2.54 (br. s, 1H), 1.97 (s, 3H), 1.95 (s, 3H), 1.74-1.72 (m, 2H), 1.62-1.60 (m, 1H), 1.49 (s, 9H), 1.33- 1.23 (m, 5H), 1.19-1.11 (m, 3H) ppm. ^{13}C NMR (100 MHz, CDCl3) δ 167.9, 157.3, 132.7, 129.4, 128.3, 125.8, 117.6, 115.0, 106.4, 82.6, 66.0, 56.6, 42.8, 33.5, 29.8, 28.1, 26.3, 25.2, 12.8, 10.7 ppm.

4.1.7.31. 2-(4-(3-((cyclohexylamino)methyl)-2,5-dimethyl-1H-pyrrol-1-yl)phenoxy)acetic acid (5y). Yield: 100 %. ^{1}H NMR (400 MHz, CD3OD) δ 7.14-7.12 (m, 2H), 7.10-7.07 (m, 2H), 5.50 (s, 1H), 4.81 (s, 2H), 4.31-4.25 (m, 1H), 4.05 (s, 1H), 3.82 (s, 2H), 3.12 (br. s, 1H), 2.01 (s, 3H), 1.98 (s, 3H), 1.93-1.91 (m, 2H), 1.44-1.40 (m, 2H), 1.34-1.30 (m, 5H) ppm. ^{13}C NMR (100 MHz, CD3OD) δ 171.2, 159.4, 133.3, 130.8, 130.6, 130.1, 125.5, 116.5, 110.0, 66.2, 57.3, 52.7, 41.8, 35.7, 30.4, 26.2, 25.6, 12.9, 10.9 ppm. HRMS: m/z (ESI) calculated for $C_{21}H_{27}N_2O_3^-$ 355.2027, found: 355.2033 $[M - H]^-$.

4.1.7.32. ethyl 4-(3-((cyclohexylamino)methyl)-2,5-dimethyl-1H-pyrrol-1-yl)benzoate (5z): Yield 42 %. ^{1}H NMR (400 MHz, CDCl3) δ 9.41 (br. s, 1H), 8.12 (d, *J* = 8.5 Hz, 2H), 7.21 (d, *J* = 8.5 Hz, 2H), 6.34 (s, 1H), 4.41 (q, *J* = 7.1 Hz, 2H), 3.90 (s, 2H), 2.99-2.92 (m, 1H), 2.26-2.20 (m, 2H), 2.04 (s, 3H), 1.97 (s, 3H), 1.72-1.58 (m, 6H), 1.41 (d, *J* = 7.1 Hz, 2H), 1.25-1.22 (m, 3H) ppm. ^{13}C NMR (100 MHz, CDCl3) δ 165.9, 142.5, 130.7, 130.2, 129.0, 128.7, 128.3, 109.0, 61.5, 54.6, 39.6, 29.2, 25.0, 24.7, 14.5, 13.0, 11.3 ppm. HRMS: m/z (ESI) calculated for $C_{22}H_{31}N_2O_2^+$ 355.2328, found: 355.2321 $[M + H]^+$.

4.1.7.33. tert-butyl 4-(3-((cyclohexylamino)methyl)-2,5-dimethyl-1H-pyrrol-1-yl)benzoate (17). Yield: 45 %. ^{1}H NMR (400 MHz, CDCl3) δ 8.07 (d, *J* = 8.4 Hz, 2H), 7.23 (d, *J* = 8.4 Hz, 2H), 6.01 (s, 1H), 3.67 (s, 2H), 2.64-2.58 (m, 1H), 2.00 (s, 3H), 1.99 (s, 3H), 1.98-1.95 (m, 2H), 1.79-1.74 (m, 2H), 1.30-1.19 (m, 6H) ppm.

4.1.7.34. 4-(3-((cyclohexylamino)methyl)-2,5-dimethyl-1H-pyrrol-1-yl)benzoic acid (5aa). Yield 100 %. ^{1}H NMR (400 MHz, CD3OD) δ 8.18 (d, *J* = 8.1 Hz, 2H), 7.32 (d, *J* = 8.4 Hz, 2H), 5.49 (s, 1H), 4.06 (br. s, 2H), 3.11 (br. s, 1H), 2.21-2.17 (m, 2H), 2.05 (s, 3H), 2.02 (s, 3H), 1.91-1.87 (m, 2H), 1.75-1.70 (m, 2H), 1.45-1.37 (m, 4H) ppm. ^{13}C NMR (100 MHz,

CD$_3$OD) δ 168.8, 143.7, 132.0, 130.4, 129.6, 129.5, 110.8, 57.4, 41.7, 30.4, 26.1, 25.5, 12.8, 10.8 ppm. HRMS: m/z (ESI) calculated for C$_{20}$H$_{25}$N$_2$O$_2^-$ 325.1922, found: 325.1821 [M - H]$^-$.

4.1.7.35.   tert-butyl   (4-(((1-(4-chlorophenyl)-2,5-dimethyl-1H-pyrrol-3-yl)methyl)amino)cyclohexyl)carbamate (5ab intermediate). Yield: 57 %. ^{1}H NMR (400 MHz, CDCl$_3$) δ 7.42 (d, J = 8.7 Hz, 2H), 7.09 (d, J = 8.5 Hz, 2H), 6.21 (s, 1H), 4.33 (br. s, 1H), 3.89 (s, 2H), 3.46 (br. s, 1H), 2.93 (br. s, 1H), 2.29-2.24 (m, 2H), 2.13-2.07 (m, 2H), 2.01 (s, 3H), 1.95 (s, 3H), 1.82-1.70 (m, 4H), 1.43 (s, 9H) ppm. ^{13}C NMR (100 MHz, CDCl$_3$) δ 158.4, 155.0, 149.4, 137.0, 134.2, 131.7, 129.7, 129.2, 128.8, 108.3, 77.4, 48.6, 40.1, 32.1, 29.8, 29.5, 28.5, 27.9, 12.9, 11.2 ppm.

4.1.7.36.   N^1-((1-(4-chlorophenyl)-2,5-dimethyl-1H-pyrrol-3-yl)methyl)cyclohexane-1,4-diamine (5ab). Yield 100 %. ^{1}H NMR (400 MHz, CD$_3$OD) δ 7.52 (d, J = 7.8 Hz, 2H), 7.21 (d, J = 8.0 Hz, 2H), 6.09 (s, 1H), 4.08 (s, 2H), 3.22 (br. s, 2H), 2.35-2.20 (m, 4H) 2.04 (s, 3H), 1.99 (s, 3H), 1.68-1.55 (m, 4H) ppm. ^{13}C NMR (100 MHz, CD$_3$OD) δ 138.3, 135.3, 131.0, 130.7, 130.4, 129.8, 110.3, 55.7, 42.4, 30.7, 29.6, 28.0, 12.7, 10.9 ppm. HRMS: m/z (ESI) calculated for C$_{19}$H$_{27}$ClN$_3^+$ 332.1888, found: 332.1903 [M + H]$^+$.

4.2. Biology

4.2.1. Minimum inhibitory concentration

The minimum inhibitory concentration (MIC$_{90}$) is the concentration at which 90% of mycobacterial growth was inhibited compared to an untreated control. The mycobacteria were cultivated in 7H9 medium added 10% OADC (oleic acid, albumin, dextrose, and catalase). In a 96-well plate, the compounds, and the antibiotics (MOX, RIF, INH and AMK) were serially diluted (0.10-25 µg/mL – 100 µL). The mycobacterium inoculum was adjusted to ~10^6 CFU/mL and the volume of 100 µL was added to the wells. After seven days, resazurin (0.01% - 30 µL) was added as the indicator of bacteria viability [33,34].

4.2.2. Cytotoxicity assay

The cytotoxicity index (IC$_{50}$) is the concentration with 50% viable cells according to an experimental control without any treatment. Murine macrophages (lineage J774A.1 ATCC TIB-67) were cultured in RPMI medium with 10% fetal bovine serum (FBS) and human pulmonary fibroblasts (MRC-5 cell line - ATCC CCL-171) in DMEM medium with 10% FBS (37 °C and 5% CO$_2$).

Cells were grown in bottles and then seeded in 96-well plates (5×10^5 cells/mL - 100 µL). One day later, the compounds were added and serially diluted (0.39-100 µg/mL) in fresh medium. After 24 h, the treatment was removed and resazurin solution was added as the cell viability indicator [35]. The same procedure was performed during 72 h to define the non-toxic concentrations for the intramacrophage assay of infection and treatment. The selectivity index (SI) is calculated by the IC_{50}/MIC_{90} ratio and SI represents how much a compound can eliminate the microorganism without causing mammalian cell damage. Thus, higher SI values are considered promising [36].

4.2.3. Time-kill

In 125 mL Erlenmeyer flasks, the *M. tuberculosis* H37Rv bacillar suspension (50mL) was added at approximately 10^6 CFU/mL. The compounds and antibiotic were added (1xMIC) and the flasks incubated at 37 °C in a shaker. Aliquots (100 µL) were regularly recovered at 1st, 2nd, 3rd, 6th, 9th, and 12th day. A serial decimal dilution was performed and aliquots (100 µL) of each dilution were plated on 7H11 solid medium plates supplemented with 10% of OADC. These plates were incubated until the colonies were counted at 37 °C, with 5% CO_2. The experiment was performed in biological duplicate and the results expressed in Log_{10} CFU/mL (mean ± standard deviation) versus time (days) [22].

4.2.4. Intramacrophagic activity

The murine macrophages (J774A.1) cell concentration was adjusted to 5×10^5 cells/mL and 1 mL of this suspension was added to a 24 well plate. After 24 h for macrophages adhesion, the mycobacterial suspension was added for phagocytosis. *M. tuberculosis* inoculum was adjusted to ~10^6 CFU/mL (RPMI medium + 10% FBS). After 2 h, to remove the extracellular mycobacteria, three successive washes with phosphate-buffer saline (PBS) were made. Then, the treatment was added at concentrations non-toxic to the macrophage in 72 h (previously determined). This treatment remained in contact with the infected cells for 72 h in incubation at 37 °C with 5% CO_2. After this time, the supernatant was discarded, the cells washed with PBS and then the macrophages had their membranes ruptured with Triton 0.1%. The intramacrophagic content was diluted and seeded onto solid media plates (7H11 with 10% OADC). The plates were incubated at 37 ºC until the colonies were counted. Results are displayed as the percentage of inhibition of mycobacterial growth relative to an untreated control [34].

4.3. Computational – Molecular docking

The cryo-EM of MmpL3 (entry 7nvh of the protein data bank, 3.0 Å resolution) was obtained from the protein data bank and prepared according to the Protein Preparation Wizard procedure from Schrodinger suite, release 2019-2 [37]. The structures of the ligands were sketched and then converted into 3D structures with the LigPrep routine, considering possible tautomeric states and protonation at pH 7 ± 1. The induced fit docking protocol [38] was used to determine the scores and the poses of the ligands. The grid was defined selecting the key amino acids of the cavity (Asp640, Tyr641, Asp251, Tyr252), resulting in a box of 30 Å for each side. A 34 Å thick membrane (numerical value taken from ref. 25) was placed in the trans-helical region of MmpL3 for consistency. The structures were docked using 0.5 van der Waals scaling for both the ligand and the receptor. The same structures were afterwards re-docked using extra precision (XP) Glide scoring function with default parameters [39]. Amide bonds within the grid were allowed to vary their conformation. Side chains of amino acids within 5 Å from the ligand were optimized and refined using Prime software. At the end, a maximum of 20 poses per ligand were retained. The interaction between ligands and the receptor were generated with the Ligand Interaction Visualization tool within Maestro interface.

Acknowledgements

Appendix A. Supplementary data

Supplementary data to this article can be found

Author contributions

The manuscript was written through contributions of all authors. All authors have given approval to the final version of the manuscript.

References

[1]   Global tuberculosis report 2021. Geneva: World Health Organization; 2021. Licence: CC BY-NC-SA 3.0 IGO. https://www.who.int/publications/i/item/9789240037021.

[2]   A. Mabhula, V. Singh, Drug-resistance in Mycobacterium tuberculosis: Where we stand, Medchemcomm. 10 (2019) 1342–1360. doi:10.1039/c9md00057g.

[3]   B.A. Sheikh, B.A. Bhat, U. Mehraj, W. Mir, S. Hamadani, M.A. Mir, Development of New Therapeutics to Meet the Current Challenge of Drug Resistant Tuberculosis, Curr. Pharm. Biotechnol. 22 (2020) 480–500. doi:10.2174/1389201021666200628021702.

[4]   L. Nguyen, Antibiotic resistance mechanisms in M. tuberculosis: an update, Arch. Toxicol. 90 (2017) 1585–1604. doi:10.1007/s00204-016-1727-6.

[5]   A. Sharma, M. De Rosa, N. Singla, G. Singh, R.P. Barnwal, A. Pandey, Tuberculosis: An Overview of the Immunogenic Response, Disease Progression, and Medicinal Chemistry Efforts in the Last Decade toward the Development of Potential Drugs for Extensively Drug-Resistant Tuberculosis Strains, J. Med. Chem. 64 (2021) 4359–4395. doi:10.1021/acs.jmedchem.0c01833.

[6]   S. Tiberi, N. du Plessis, G. Walzl, M.J. Vjecha, M. Rao, F. Ntoumi, S. Mfinanga, N. Kapata, P. Mwaba, T.D. McHugh, G. Ippolito, G.B. Migliori, M.J. Maeurer, A. Zumla, Tuberculosis: progress and advances in development of new drugs, treatment regimens, and host-directed therapies, Lancet Infect. Dis. 18 (2018) e183–e198. doi:10.1016/S1473-3099(18)30110-5.

[7]   D. Bald, C. Villellas, P. Lu, A. Koul, Targeting Energy Metabolism in Mycobacterium tuberculosis, a New Paradigm in Antimycobacterial Drug Discovery, mBio. 8 (2017) 1–11. doi: 10.1128/mBio.00272-17.

[8]   Global tuberculosis report 2020. Geneva: World Health Organization; 2020. Licence: CC BY-NC-SA 3.0 IGO. https://www.who.int/publications/i/item/9789240013131.

[9]   World Health Organization 2020 Meeting Report of the WHO Expert Consultation on the Definition of Extensively Drug-Resistant Tuberculosis, Meet. Rep. WHO Expert Consult. Defin. Extensively Drug-Resistant Tuberc. (2020). https://www.who.int/publications/i/item/meeting-report-of-the-who-expert-consultation-on-the-definition-of-extensively-drug-resistant-tuberculosis.

[10]   Stop TB Partnership Working Group on New TB Drugs. https://www.newtbdrugs.org/.

[11]   A.A. Adeniji, K.E. Knoll, D.T. Loots, Potential anti-TB investigational compounds and drugs with repurposing potential in TB therapy: a conspectus, Appl. Microbiol. Biotechnol. 104 (2020) 5633–5662. doi: 10.1007/s00253-020-10606-y.

[12]   D. Machado, M. Girardini, M. Viveiros, M. Pieroni, Challenging the drug-likeness dogma for new drug discovery in Tuberculosis, Front. Microbiol. 9 (2018). doi:10.3389/fmicb.2018.01367.

[13]   R. Bairwa, M. Kakwani, N.R. Tawari, J. Lalchandani, M.K. Ray, M.G.R. Rajan, M.S. Degani, Novel molecular hybrids of cinnamic acids and guanylhydrazones as potential antitubercular agents, Bioorg. Med. Chem. Lett. 20 (2010) 1623–1625. doi:10.1016/j.bmcl.2010.01.031.

[14]   A.B. Danne, A.S. Choudhari, S. Chakraborty, D. Sarkar, V.M. Khedkar, B.B. Shingate, Triazole-diindolylmethane conjugates as new antitubercular agents: synthesis, bioevaluation, and molecular docking, Medchemcomm. 9 (2018) 1114–1130. doi:10.1039/c8md00055g.

[15] G.F. Dos Santos Fernandes, C.M. Chin, J.L. Dos Santos, Advances in drug discovery of new antitubercular multidrug-resistant compounds, Pharmaceuticals. 10 (2017) 1–17. doi:10.3390/ph10020051.

[16] A. Maitra, S.D.S. Bates, M. Shaik, Di. Evangelopoulos, I. Abubakar, T.D. McHugh, M. Lipman, S. Bhakta, Repurposing drugs for treatment of tuberculosis: A role for non-steroidal anti-inflammatory drugs, Br. Med. Bull. 118 (2016) 138–148. doi:10.1093/bmb/ldw019.

[17] R.S. Wallis, M. Maeurer, P. Mwaba, J. Chakaya, R. Rustomjee, G.B. Migliori, B. Marais, M. Schito, G. Churchyard, S. Swaminathan, M. Hoelscher, A. Zumla, Tuberculosis-advances in development of new drugs, treatment regimens, host-directed therapies, and biomarkers, Lancet Infect. Dis. 16 (2016) e34–e46. doi:10.1016/S1473-3099(16)00070-0.

[18] S. Bhakta, N. Scalacci, A. Maitra, A.K. Brown, S. Dasugari, D. Evangelopoulos, T.D. McHugh, P.N. Mortazavi, A. Twist, E. Petricci, F. Manetti, D. Castagnolo, Design and Synthesis of 1-((1,5-Bis(4-chlorophenyl)-2-methyl-1H-pyrrol-3-yl)methyl)-4-methylpiperazine (BM212) and N-Adamantan-2-yl-N′-((E)-3,7-dimethylocta-2,6-dienyl)ethane-1,2-diamine (SQ109) Pyrrole Hybrid Derivatives: Discovery of Potent Antitubercul, J. Med. Chem. 59 (2016) 2780–2793. doi:10.1021/acs.jmedchem.6b00031.

[19] D. Masci, C. Hind, M.K. Islam, A. Toscani, M. Clifford, A. Coluccia, I. Conforti, M. Touitou, S. Memdouh, X. Wei, G. La Regina, R. Silvestri, J.M. Sutton, D. Castagnolo, Switching on the activity of 1,5-diaryl-pyrrole derivatives against drug-resistant ESKAPE bacteria: Structure-activity relationships and mode of action studies, Eur. J. Med. Chem. 178 (2019) 500–514. doi:10.1016/j.ejmech.2019.05.087.

[20] M. Touitou, F. Manetti, C.M. Ribeiro, F.R. Pavan, N. Scalacci, K. Zrebna, N. Begum, D. Semenya, A. Gupta, S. Bhakta, T.D. McHugh, H. Senderowitz, M. Kyriazi, D. Castagnolo, Improving the Potency of N-Aryl-2,5-dimethylpyrroles against Multidrug-Resistant and Intracellular Mycobacteria, ACS Med. Chem. Lett. (2019). doi:10.1021/acsmedchemlett.9b00515.

[21] D. Semenya, M. Touitou, C.M. Ribeiro, F.R. Pavan, L. Pisano, V. Singh, K. Chibale, G. Bano, A. Toscani, F. Manetti, B. Gianibbi, D. Castagnolo, Structural Rigidification of N-Aryl-pyrroles into Indoles Active against Intracellular and Drug-Resistant Mycobacteria, ACS Med. Chem. Lett. (2021). doi:10.1021/acsmedchemlett.1c00431.

[22] J.E.M. de Steenwinkel, G.J. de Knegt, M.T. ten Kate, A. van Belkum, H.A. Verbrugh, K. Kremer, D. van Soolingen, I.A.J.M. Bakker-Woudenberg, Time-kill kinetics of anti-tuberculosis drugs, and emergence of resistance, in relation to metabolic activity of Mycobacterium tuberculosis, J. Antimicrob. Chemother. 65 (2010) 2582–2589. doi:10.1093/jac/dkq374.

[23] A. Naidoo, K. Naidoo, H. Mcilleron, S. Essack, N. Padayatchi, A review of moxifloxacin for the treatment of drug-susceptible tuberculosis, J. Clin. Pharmacol. 57 (2018) 1369–1386. doi:10.1002/jcph.968.A.

[24] J. Gawad, C. Bonde, Current Affairs, Future Perspectives of Tuberculosis and Antitubercular Agents, Indian J. Tuberc. 65 (2018) 15–22. doi:10.1016/j.ijtb.2017.08.011.

[25] O. Adams, J.C. Deme, J.L. Parker, CRyPTIC Consortium, P.W. Fowler, S.M. Lea, S. Newstead, Cryo-EM structure and resistance landscape of M. tuberculosis MmpL3: An emergent therapeutic target, Structure. 29 (2021) 1182–1191. https://doi.org/10.1016/j.str.2021.06.013.

[26] H. Cho, R. Madden, B. Nisanci, B. Török, The Paal–Knorr reaction revisited. A catalyst and solvent-free synthesis of underivatized and N-substituted pyrroles, Green Chem. 17 (2015) 1088–1099. https://doi.org/10.1039/C4GC01523A.

[27] N. Scalacci, G.W. Black, G. Mattedi, N.L. Brown, N.J. Turner, D. Castagnolo, Unveiling the Biocatalytic Aromatizing Activity of Monoamine Oxidases MAO-N and 6-HDNO: Development of Chemoenzymatic Cascades for the Synthesis of Pyrroles, ACS Catal. 7 (2017) 1295–1300. https://doi.org/10.1021/acscatal.6b03081

[28] S.J. Pridmore, P.A. Slatford, J.E. Taylor, M.K. Whittlesey, J.M.J. Williams, Synthesis of furans, pyrroles and pyridazines by a ruthenium-catalysedisomerisation of alkynediols and in situ cyclisation, Tetrahedron. 65 (2009) 8981–8986. https://doi.org/10.1016/j.tet.2009.06.108.

[29]   X. Chen, M. Yang, M. Zhou, Efficient synthesis of substituted pyrroles through Pd(OCOCF3)2-catalyzed reaction of 5-hexen-2-one with primary amines, Tetrahedron Lett. 57 (2016) 5215–5218. https://doi.org/10.1016/j.tetlet.2016.10.029.

[30]   A.E. Williamson, P.M. Ylioja, M.N. Robertson, Y. Antonova-Koch, V. Avery, J.B. Baell, H. Batchu, S. Batra, J.N. Burrows, S. Bhattacharyya, F. Calderon, S.A. Charman, J. Clark, B. Crespo, M. Dean, S.L. Debbert, M. Delves, A.S.M. Dennis, F. Deroose, S. Duffy, S. Fletcher, G. Giaever, I. Hallyburton, F.-J. Gamo, M. Gebbia, R.K. Guy, Z. Hungerford, K. Kirk, M.J. Lafuente-Monasterio, S.M. Anna Leeη, C. Nislow, J.P. Overington, G. Papadatos, L. Patiny, J. Pham, S.A. Ralph, A. Ruecker, E. Ryan, C. Southan, K. Srivastava, C. Swain, M.J. Tarnowski, P. Thomson, P. Turner, I.M. Wallaceι, T.N.C. Wells, K. White, L. White, P. Willis, E.A. Winzeler, S. Wittlin, M.H. Todd, Open Source Drug Discovery: Highly Potent Antimalarial Compounds Derived from the Tres Cantos Arylpyrroles, ACS Cent. Sci. 2 (2016) 687–701. https://doi.org/10.1021/acscentsci.6b00086.

[31]   S.D. Joshi, D. Kumar, U.A. More, K.S. Yang, T.M. Aminabhavi, Design and development of pyrrole carbaldehyde: an effective pharmacophore for enoyl-ACP reductase, Med. Chem. Res. 25 (2016) 672–689. https://doi.org/10.1007/s00044-016-1517-y.

[32]   F. Manetti, M. Magnani, D. Castagnolo, L. Passalacqua, M. Botta, F. Corelli, M. Saddi, D. Deidda, A. De Logu, Ligand-based virtual screening, parallel solution-phase and microwave-assisted synthesis as tools to identify and synthesize new inhibitors of Mycobacterium tuberculosis, ChemMedChem. 1 (2006) 973–989. doi:10.1002/cmdc.200600026.

[33]   J. Palomino, A. Martin, M. Camacho, H. Guerra, J. Swings, F. Portaels, Resazurin Microtiter Assay Plate : Simple and Inexpensive Method for Detection of Drug Resistance in Mycobacterium tuberculosis Resazurin Microtiter Assay Plate : Simple and Inexpensive Method for Detection of Drug Resistance in Mycobacterium tuberculosis, Antimicrob. Agents Chemother. 46 (2002) 2720–2722. doi:10.1128/AAC.46.8.2720.

[34]   G.F. Dos Santos Fernandes, P.C. De Souza, E. Moreno-Viguri, M. Santivañez-Veliz, R. Paucar, S. Pérez-Silanes, K. Chegaev, S. Guglielmo, L. Lazzarato, R. Fruttero, C. Man Chin, P.B. Da Silva, M. Chorilli, M.C. Solcia, C.M. Ribeiro, C.S.P. Silva, L.B. Marino, P.L. Bosquesi, D.M. Hunt, L.P.S. De Carvalho, C.A. De Souza Costa, S.H. Cho, Y. Wang, S.G. Franzblau, F.R. Pavan, J.L. Dos Santos, Design, Synthesis, and Characterization of N-Oxide-Containing Heterocycles with in Vivo Sterilizing Antitubercular Activity, J. Med. Chem. 60 (2017) 8647–8660. doi:10.1021/acs.jmedchem.7b01332.

[35]   I.C. Silva, C.R. Polaquini, L.O. Regasini, H. Ferreira, F.R. Pavan, Evaluation of cytotoxic , apoptotic , mutagenic , and chemopreventive activities of semi-synthetic esters of gallic acid, Food Chem. Toxicol. 105 (2017) 300–307. doi:10.1016/j.fct.2017.04.033.

[36]   S. Ekins, R.C. Reynolds, H. Kim, M.S. Koo, M. Ekonomidis, M. Talaue, S.D. Paget, L.K. Woolhiser, A.J. Lenaerts, B.A. Bunin, N. Connell, J.S. Freundlich, Bayesian models leveraging bioactivity and cytotoxicity information for drug discovery, Chem. Biol. 20 (2013) 370–378. doi:10.1016/j.chembiol.2013.01.011.

[37]   Schrödinger Release 2019-2. Schrödinger, LLC, New York, NY, 2019.

[38]   W. Sherman, T. Day, M. P. Jacobson, R. A. Friesner, R. Farid, Novel Procedure for Modeling Ligand/Receptor Induced Fit Effects. J. Med. Chem. 49 (2006) 534-553. https://doi.org/10.1021/jm050540c.

[39]   R. A. Friesner, R. B. Murphy, M. P. Repasky, L. L. Frye, J. R. Greenwood, T. A. Halgren, P. C. Sanschagrin, D. T. Mainz, Extra Precision Glide: Docking and Scoring Incorporating a Model of Hydrophobic Enclosure for Protein-Ligand Complexes. *J. Med. Chem.* 49 (2006) 6177-6196. https://doi.org/10.1021/jm051256o.

GRAPHICAL ABSTRACT

MIC = **0.73** μg/mL   MIC = **0.40** μg/mL